



A Review on Advanced Strengthening Techniques for Corrosion-Damaged Reinforced Concrete Structures

Mankare Ulka Shesharao ¹; Viswanathan T.S ^{2,*} 

1. Ph.D. Candidate, Department of Structural and Geotechnical Engineering, Vellore Institute of Technology University, Vellore, 632014, Tamilnadu, India

2. Associate Professor, Department of Structural and Geotechnical Engineering, Vellore Institute of Technology University, Vellore, 632014, Tamilnadu, India

* Corresponding author: viswanathan.ts@vit.ac.in

ARTICLE INFO

Article history:

Received: 10 May 2025

Revised: 30 July 2025

Accepted: 17 August 2025

Keywords:

Reinforced concrete;

Corrosion;

Fiber Reinforced Polymer;

Retrofitting;

Flexural behavior.

ABSTRACT

Corrosion of steel reinforcement in reinforced concrete (RC) structures causes an appreciable loss of mechanical properties, which subsequently affects load-carrying capacity, durability, and structural safety. More than 63 scientific papers, including experimental, field based and computational, investigations on the behavior of corroded Reinforced Concrete beams, slabs, and columns strengthened with high-performance materials published between 2003 to 2024 are critically examined in the present study. Engineered Cementitious Composites (ECC), Ultra high-Performance Concrete (UHPC), Fibre reinforced polymers (FRP), and Hybrid systems are the major categories to which the examined methods belong. FRP-based methods such as CFRP laminates, NSM reinforcements, and jackets significantly enhanced flexural and shear strength. Although hybrid methods such as Impressed Current Cathodic Protection-Structural Strengthening (ICCP-SS) and Cementitious Fiber Reinforced Composite Material (C-FRCM) systems provided advantages for both mechanical and corrosion protection, UHPC overlays and ECC wraps improved ductility, crack control, and durability. Finite element modeling and parametric studies validated such enhancements with predictive precision. In spite of these advances, problems like interface debonding, long-term performance under combined corrosion-loading conditions, and absence of standard retrofit design codes continue to exist. This review identifies research gaps in cyclic behavior under environmental stressors, long-term performance modelling, and cost-efficient hybrid solutions. Future studies are suggested to aim at evolving multi-functional, long-lasting, and sustainable strengthening approaches complemented by advanced simulation and monitoring technologies.

E-ISSN: 2345-4423

© 2025 The Authors. Journal of Rehabilitation in Civil Engineering published by Semnan University Press.

This is an open access article under the CC-BY 4.0 license. (<https://creativecommons.org/licenses/by/4.0/>)

How to cite this article:

Mankare Ulka Shesharao and Viswanathan T.S (2026). A review on Advanced strengthening techniques for corrosion-damaged Reinforced Concrete structures. Journal of Rehabilitation in Civil Engineering, 14(2), 2340.

<https://doi.org/10.22075/jrce.2025.2340>

1. Introduction

Reinforced concrete (RC) members are the fundamental components of modern infrastructure due to their cost-effectiveness and structural reliability. They are extensively used in buildings, bridges, and transportation systems. But one of the most significant problems posing a threat to the durability and safety of RC structures is embedded steel corrosion. Corrosion substantially worsens the mechanical behavior of RC members, decreasing their flexural and shear strength, stiffness, and ductility, thus raising the structural failure risk [1–3]. The issue is particularly common in city life where de-icing salts and industrial contaminants advance reinforcement degradation, and in harsh marine environments where chloride penetration enhances steel corrosion [4–6]. The subsequent damage i.e., cracking of the concrete cover and degradation of bond strength between concrete and steel can result in premature failure, particularly under seismic, impact, and cyclic loading conditions [7–10]. The imperative of creating efficient and sustainable rehabilitation methods is emphasized by the projected worldwide cost of \$1.8 trillion per year to repair deteriorated RC structures [1].

To mitigate these issues, researchers have proposed several new strengthening and retrofitting methods. Among these, Fiber Reinforced Polymers (FRP) such as Carbon Fiber Reinforced Polymer (CFRP) and Basalt Fiber Reinforced Polymer (BFRP) have received considerable interest because of their high strength-to-weight ratios, resistance to corrosion, and simplicity of application [11–14]. FRP systems externally bonded (EB) sheets and near-surface mounted (NSM) laminates have been used successfully to rehabilitate or enhance the flexural and shear capacity of corroded RC slabs, beams, and columns [14,15]. Concurrently, advanced cementitious composites such as ultra-high-performance concrete (UHPC) and engineered cementitious composites (ECC) have also been highly promising. UHPC provides high compressive strength and durability and is thus a good material to be used for retrofitting corroded structures [5,9,16,17], whereas ECC provides strain-hardening behavior and improved crack control and is hence useful in long-term retrofitting applications [4,18].

Recent advancements have resulted in the availability of hybrid strengthening systems combining FRPs with other high-performance materials like ultra-high toughness cementitious composites (UHTCC) and textile-reinforced concrete (TRC). These hybrid techniques present better bond properties, effective load transfer, and increased resistance to environmental degradation [17,19,20]. Additionally, application of CFRP rods, anchor bolts, and other mechanical fasteners has been investigated to reduce premature debonding of externally bonded reinforcements [1,21]. One highly promising innovation is the combination of structural strengthening and corrosion protection systems, e.g., Impressed Current Cathodic Protection (ICCP) with carbon fabric-reinforced cementitious matrices (C-FRCM), providing both mechanical strengthening and corrosion protection [22–24].

Numerous experimental programs, numerical analyses, and analytical models have been created to evaluate and predict the performance of corroded and retrofitted RC members. Finite element analysis (FEA) has been extensively applied to model the sophisticated degradation and failure processes under various loading conditions, allowing for precise predictions of structural behavior [25–28]. Experimental investigations have confirmed these models and offered significant insight into optimal strengthening methods for RC slabs, beams, and columns [8,29]. Long-term information has also been derived on the seismic, cyclic, and in-plane loading performance of strengthened members [7,10].

In spite of all these developments, there are a number of challenges still to be addressed. Debonding between the FRP and concrete, long-term performance under combined mechanical and environmental load, and the absence of standardized specifications for retrofitting corroded RC members hinder the extensive adoption of these methods [21]. In addition, the long-term cyclic response of FRP-retrofitted corroded members and modeling of corrosion-induced deterioration through precise predictive models are topics that need to be investigated further.

Structural Health Monitoring (SHM) plays a key role in the premature detection, assessment, and control of degradation in reinforced concrete (RC) structures, especially those suffering from corrosion. SHM

systems employ an assortment of sensing technologies such as fiber optic sensors, piezoelectric sensors, acoustic emission, and corrosion monitoring probes for real-time reporting of the structural condition and corrosion activity. This facilitates more effective identification of deteriorated areas, enabling targeted strengthening and optimal resource utilization. SHM also facilitates continuous monitoring of repaired or retrofitted structures to ensure that strengthening methods utilized are effective under service loads. Integration of SHM in rehabilitation planning optimizes the safety and service life of RC structures. Recent research has demonstrated the application of SHM techniques in structural components and systems, with potential relevance to corrosion-related damage [30–33].

This review critically examines twenty-one experimentally validated strengthening techniques for corrosion-damaged reinforced concrete (RC) structures, systematically categorizing them into fiber-reinforced polymer (FRP), cementitious, hybrid, and textile-based systems. The objective is to provide a comprehensive evaluation of these methods by comparing their effectiveness through experimental and numerical studies. In doing so, the review identifies current research gaps and offers informed recommendations to guide the development of robust, durable, and cost-effective retrofitting strategies for aging RC infrastructure.

2. Methodology

To ensure a structured and comprehensive review of the literature on strengthening techniques for corroded reinforced concrete (RC) members, a systematic approach was adopted in accordance with established review protocols.

2.1. Database selection

The following major academic databases were utilized to gather relevant peer-reviewed publications: Scopus, Web of Science, ScienceDirect, Google Scholar, ASCE Library, SpringerLink, Taylor & Francis Online, IEEE Xplore.

2.2. Search strategy and keywords

A structured keyword search was implemented using Boolean operators. The search strings included combinations of the following terms: corrosion-damaged concrete, reinforced concrete, corrosion, structural strengthening techniques, FRP, CFRP, GFRP, NSM, FRCM, UHPC, ECC, ICCP, hybrid systems, RC beams/slabs/columns and retrofitting, post-corrosion performance, flexural, shear, fatigue, ductility and corrosion, durability and rehabilitation.

2.3. Inclusion and exclusion criteria

Included criteria:

- Peer-reviewed articles or conference proceedings from reputable sources.
- Research exclusively on corroded RC member strengthening techniques.
- Papers presenting experimental, numerical, or hybrid analyses.

Research assessing major performance indicators like load-carrying capacity, ductility, crack control, or durability.

Excluded criteria:

- Studies focused solely on corrosion detection or prevention without post-corrosion strengthening.
- Papers not available in full text.
- Articles in a non-English language without a verified translation.
- Case studies lacking performance data or scientific methodology.

2.4. Time frame

Publications from January 2000 through May 2025 were included, highlighting recent trends with a view to also including original works that laid the foundation for the area

2.5. Screening and selection process

A three-stage screening was carried out

1. Title and abstract screening to eliminate clearly irrelevant studies.
2. Review of full texts to determine relevance to post-corrosion strengthening of RC members.
3. Cross-referencing from shortlisted articles to spot other important studies.

A total of more than 200 papers were screened, and 62 most critical articles were chosen for detailed analysis and inclusion based on technical quality, relevance, and contribution to the state of the art.

3. Strengthening techniques

Reinforced concrete structures require strengthening techniques to regain their structural integrity and extend service life. To combat the corrosion-induced deterioration, various strengthening techniques have been developed and validated through experimental and Numerical techniques. These methods vary in terms of types of material, mechanism of improvement, ease of application, and durability under environmental stressors. The methods examined in this paper are divided into four categories: Fibre reinforced polymer (FRP) based strengthening techniques, Cementitious composite-based techniques, Hybrid systems and electrochemical integration, and Textile-based strengthening techniques. The following subsections provide a detailed evaluation of each class, discussing their benefits, limitations, and implementation considerations.

3.1. FRP based strengthening techniques

3.1.1. Aljidda et al.(2023) [14]

Near Surface Mounted-Basalt Fibre Reinforced Polymer (NSM-BFRP) and Near Surface Mounted-Glass Fibre Reinforced Polymer (NSM-GFRP) bars The bars utilized in this research study are shown in Fig1.



Fig. 1. NSM–BFRP and NSM–GFRP bars were employed to reinforce and improve the structural integrity of the slabs. Adapted from Aljidda et al., (2023) [14].

First, a concrete saw with two diamond blades that were calibrated to the required groove width was used to cut longitudinal grooves into the slabs' concrete cover. A power chisel was then used to roughen the grooves' surface in order to increase the epoxy adhesive's adherence to the NSM bars. After that, trash and fine particles were removed from the grooves using compressed air and a steel brush. The ACI 440.2R [34] specifications were followed when designing the grooves' spacing and measurements. A square cross-section of twice the diameter of the NSM bars, d_b , and 2500 mm in length was present in each groove. The transverse clear lengths for slabs with two and four grooves were 200 mm and 110 mm, respectively. Both of these values greatly exceeded the ACI 440.2R recommended groove depth of 40 mm [34]. The NSM bars were carefully positioned inside the grooves and held up with tiny steel spacers to guarantee correct

alignment in the middle after epoxy adhesive was injected to half the depth of the grooves. The glue was allowed to run around the bars by gently pressing them into it. A handscraper was used to smooth the surface after more epoxy resin was added to fill in all of the grooves. In order to guarantee that the epoxy adhesive reached its maximum strength, the slabs were lastly cured for two weeks, as advised by the manufacturer. The procedure for reinforcing the slab specimens is shown in Figure 2.

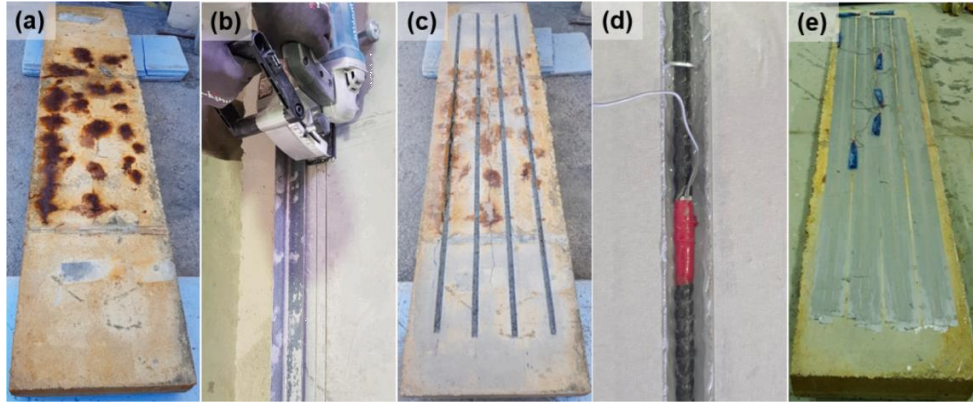


Fig. 2. illustrates the process, including: (a) a slab affected by corrosion, (b) creating grooves in the concrete using a concrete saw, (c) cleaning the grooves thoroughly, (d) inserting the NSM bars into the prepared grooves, and (e) filling the grooves with epoxy adhesive and leveling the surface. Adapted from Aljidda et al, (2023)[14].

3.1.2. Kharma et al. (2022)[27]: carbon fibre reinforced polymers (CFRP)-laminates strengthening scheme

3.1.2.1. CFRP laminates for strengthening

The corroded beam specimens were strengthened using commercial CFRP laminates. These laminates measured 0.29 mm in thickness, 3500 MPa in tensile strength, and 225 GPa in tensile modulus of elasticity. At break, the dry fiber elongation was roughly 1.7%. Wetting CFRP laminates with semi-liquid epoxy resin prior to usage is the suggested application technique [35]. Consequently, the CFRP laminates were bonded to the beam specimens using epoxy glue. The epoxy resin exhibited a 1.5% break elongation, a tensile modulus of 3500 MPa, and a flexural modulus of elasticity of 2800 MPa [36].

3.1.2.2. Strengthening beams with CFRP laminates

The CFRP laminates were cleaned with a high-pressure air jet to get rid of dust and other tiny particles before being affixed to the beam surfaces. For a stronger bond, the U-shaped CFRP laminates' edges were rounded using a grinder. To provide adequate anchorage and lower the chance of failure from debonding, these laminates were wrapped around particular sections of the beams [34,37,38]. The CFRP laminates applied to the beam surface, wrapped in U-shaped CFRP laminates, are depicted in Fig. 3. As directed by the manufacturer, the epoxy resin and hardener were combined [39]. The fibers were thoroughly soaked in the epoxy using a specialized paint roller. Following this, the CFRP laminates were affixed to the surfaces of the beams. For seven days, the beams were allowed to cure at an average temperature of 36°C. The procedures for attaching CFRP laminates to the corroded beam specimens are depicted in Fig. 4.

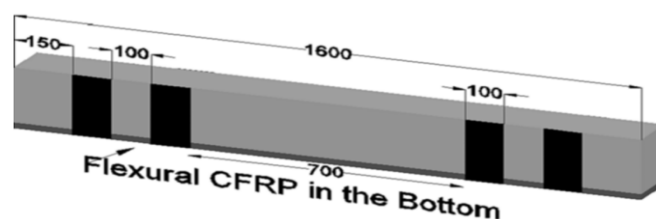


Fig. 3. Method for strengthening the corroded beams with CFRP laminates. Adapted from Kharma et al. (2022) [27].



Fig. 4. Process for applying CFRP. Adapted from Kharmah et al. (2022) [27].

3.1.3. Pan et al. (2023)[40]: carbon fibre reinforced polymers (CFRP) anchorage system strengthening

3.1.3.1. Fabrication of CFRP anchors

A few crucial stages are involved in creating CFRP anchors.[41,42] Initially, a unidirectional CFRP sheet is selected and cut to the necessary dimensions of 80 mm in length and 150 mm in width. After that, this 80 mm length is divided into two sections: a 30 mm pre-built segment with room for a 90-degree bend and a 50 mm fan-shaped section. The anchor's major component is a 10 mm dowel that is put into the fan-shaped segment. To prevent bending damage, the hardened portion of the anchor should not exceed two-thirds of the embedment length, according to Llauroadó [42]. Epoxy is applied across the entire width of a 10 mm section at the end of the sheet to produce this hardened portion. In order to create a bendable connection between the hardened part and the main body, the 30 mm pre-built segment is left flexible. Two CFRP sheets of varying lengths are cut, and the same procedures are repeated to construct the main body, hardened section, and bending section in order to create bow-tie CFRP anchors. This procedure is explained in detail in Figure 5.

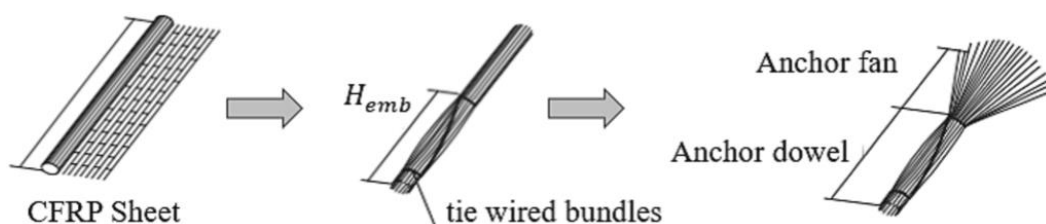


Fig. 5. depicts the process involved in constructing CFRP anchors. Adapted from Pan et al. (2023) [40].

3.1.3.2. Strengthening procedure

The Carbon Fibre Reinforced Polymers (CFRP) anchorage system strengthening process includes these steps: Surface Preparation- A pneumatic needle scaler is used to roughen the surface of the weakened concrete, exposing the aggregates beneath the top layer of concrete. This produces a rough surface that improves the adhesion of the CFRP sheets, guaranteeing the effectiveness of the reinforcement. c) Drilling Holes: A diamond-tipped drill bit (10 mm broad and 35 mm deep) is used to drill four holes into the bottom of the beams. To ensure precision, the holes' locations are indicated in advance. To ensure a proper epoxy bond, dust and debris are removed from the perforations and the beam surface using a vacuum and pressurized air. c) CFRP Sheet Application: CFRP sheets are rapidly positioned on top of epoxy resin that has been applied to the beam surface. After evenly applying a second coat of epoxy to the CFRP sheets, air

bubbles are eliminated by pressing a roller along the texture's direction. d) Anchor Installation: The CFRP anchoring rods are put into the holes that have been drilled, leaving a portion of the rod protruding from the surface of the beam. To strengthen the bond between the rod and the concrete, a tiny bit of epoxy adhesive is applied to the rods before to installation. e) Curing: To guarantee that the glue reaches its maximum strength, the adhesive and CFRP sheets are allowed to cure for around seven days, in accordance with the manufacturer's specifications.

3.1.4. Feng et al. (2022)[23]: impressed current cathodic protection-structural strengthening (ICCP-SS) and cementitious fiber reinforced composite material (C-FRCM)

3.1.4.1. Anodic polarization of C-FRCM under ICCP system

Rather of being cast in place as is customary, the C-FRCM material utilized in this investigation was supplied as a prefabricated plate. This was done to expedite the strengthening process and facilitate the direct bonding of the C-FRCM plate to the surface of the beam. The plate was intended to have two layers of cementitious matrix and one layer of carbon fiber mesh, with a thickness of 6 mm. The creation of the Cementitious Fiber Reinforced Composite Material (C-FRCM) plate is depicted in Fig. 6. The steps are as follows: First, a thick foundation plate was fixed with 3 mm thick wooden strips to produce a mold. To keep its surface clean and facilitate the eventual removal of the C-FRCM plate, the base plate was oiled. The base plate was then covered with the cementitious matrix. The mesh of carbon cloth was cut and placed over the matrix. The cementitious matrix was smoothed out to match the surrounding wooden strips, and another set of 3 mm wooden strips was placed on top. To make a multi-layer Cementitious Fiber Reinforced Composite Material (C-FRCM) plate, same procedure was repeated. Following creation, the plate was placed in a shaded area to solidify and covered with a protective coating. After the plate had hardened, the film and mold were taken off, and it was left in a regular curing room for 28 days. The entire C-FRCM plate manufacturing process is depicted in Fig. 10. A polarization device was built up to mimic the C-FRCM plate acting as the anode in the ICCP system (Fig. 7). The plate C-FRCM was To prevent the C-FRCM plate from coming into contact with the stainless steel cathode, it was encased inside an organic glass container and supported by tiny wooden blocks. A saturated calcium hydroxide and 2% sodium chloride solution was put into the container. The positive and negative poles of a power source were linked to the stainless steel plate and the C-FRCM plate, respectively. The potential of the C-FRCM plate was periodically measured throughout the test using a reference electrode.

3.1.4.2. Strengthening with prefabricated cementitious fiber reinforced composite material (c-frcm) plate

The C-FRCM plate was cut and fastened to the beam's strengthening regions after completing its anodic polarization (Fig. 8). To reveal the inner concrete layers and get rid of any contaminants, the concrete surfaces needed to be cleaned and polished before installation. To completely saturate the contact between the C-FRCM plate and the concrete, the concrete and plate were soaked for more than 24 hours. The bonding substance utilized to affix the C-FRCM plate to the concrete was the same cementitious matrix that was used to create the plate. A protective film and hydrophilic fabric were placed over the strengthening areas. The film was taken off after it had solidified for a full day. To ensure good bonding, the beams were watered twice a day for 28 days to help the cementitious matrix cure. Once curing was complete, the CFRP was applied to the beam surface using epoxy resin. After chiseling and polishing, the materials in the strengthening regions were left to naturally harden for half a day in a dry environment.

Fabrication procedures of the strengthened specimens.: Beams are fabricated and cured for 28 days. After curing, beams are watered twice daily for 11 months. Cementitious Fiber Reinforced Composite Material (C-FRCM) plates are prepared and cured for 28 days. Following curing, anodic polarization is applied to the plates for 75/90 days. Prefabricated C-FRCM plates are used to strengthen the beams. Strengthened specimens are watered twice daily for 28 days to ensure proper curing. Mechanical tests are conducted on the strengthened specimens to assess performance.



Fig. 6. Process of prefabricated C-FRCM plate. Reproduced with permission from Feng et al. (2022) [23].

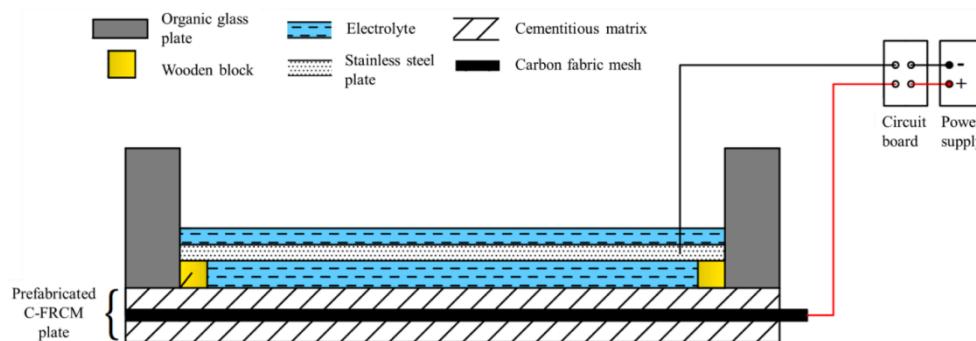


Fig. 7. Polarization setup for the prefabricated C-FRCM plate. Reproduced with permission from Feng et al. (2022)[23].



Fig. 8. Process of strengthening with prefabricated C-FRCM plate. Reproduced with permission from Feng et al. (2022)[23].

3.1.5. Sohail et al. (2024)[28] : CPRF and CFRP-GFRP Laminates

The procedure for strengthening the beam specimen details used in this study is depicted in Fig. 9. Rust spread to the tensile surface (Fig. 9a) during degradation, which could compromise the bond between the strengthening systems and the concrete beams. To address this, the underside of the beams was ground to create a smooth surface (Fig. 9b). After 15 days of applying a current of $750 \mu\text{A}/\text{cm}^2$, cracks up to 2–3 mm wide appeared on the beam's tensile surface (Fig. 9c). CFRP sheets soaked in epoxy adhesive were then carefully placed on the marked areas, another layer of epoxy was applied over the CFRP sheets, and a

steel roller was used to remove air bubbles. As advised by the manufacturer, the first adhesive layer was applied at a rate of 1 kg/m^2 , and the second layer was applied at a rate of 0.8 kg/m^2 following the placement of CFRP sheets. After the second epoxy coating, a GFRP sheet soaked in epoxy was placed on top of the CFRP sheet, and then another layer of epoxy was applied for hybrid strengthening. To eliminate air bubbles and distribute the epoxy uniformly, the steel roller was utilized once more. Beams reinforced with CFRP and CFRP-GFRP are depicted in Figs. 9d and 9e, respectively. The beams were tested under four-point bending after the epoxy had cured for two weeks.

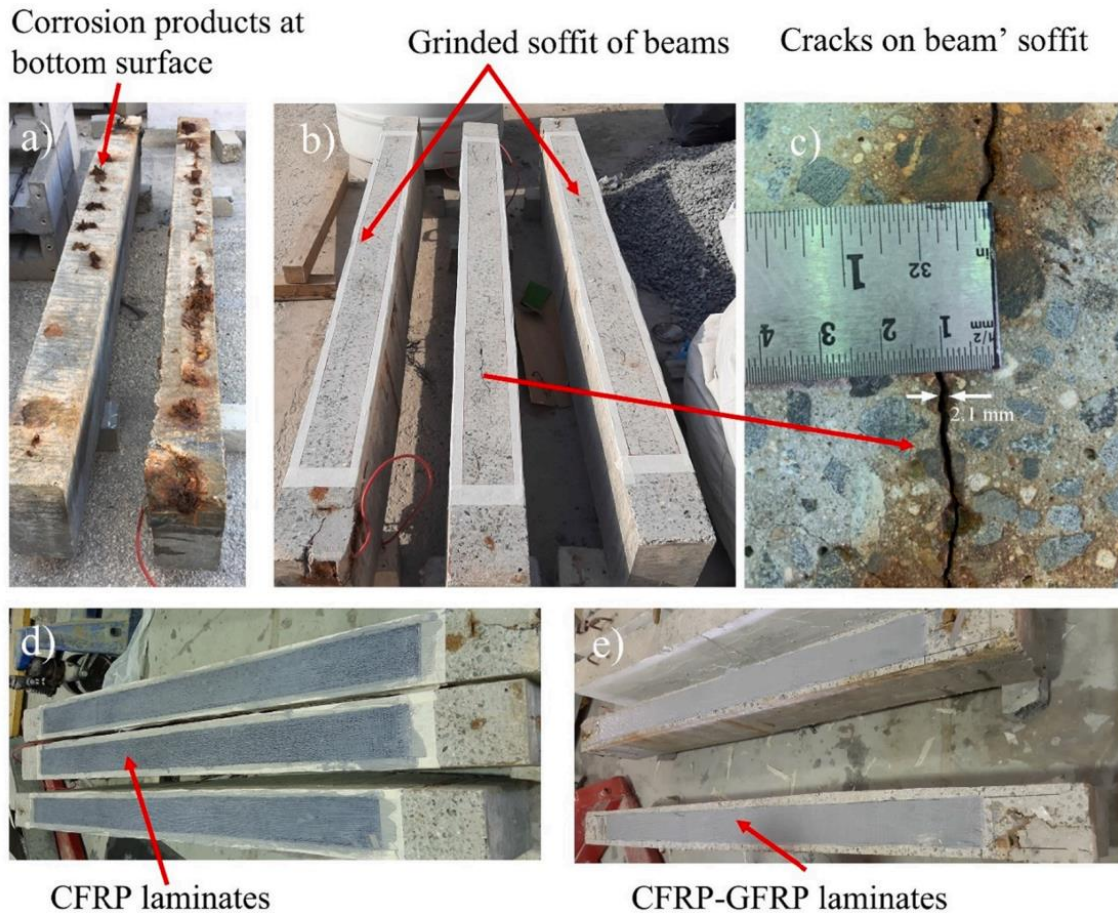


Fig. 9. Cleaning and reinforcing RC beams: a) rust products on the underside of the beams, b) the underside surface after grinding, c) corrosion cracks on the tension face up to 2-3 mm, d) CFRP-reinforced beams, and e) CFRP-GFRP laminate hybrid reinforcement. Reproduced with permission from Sohail et al. (2024)[28].

3.1.6. Karimipour et al. (2021)[7]: CFRP and GFRP fabrics

The CFRP and GFRP fabrics used in this investigation are displayed in Fig. 10. Three layers of CFRP and GFRP laminates were added to the specimens to strengthen them. The conventional externally bonded reinforcing technique was employed. Using an abrasive stone (Fig. 11a) and a grinding machine, the weak concrete layer was first eliminated. The laminates were affixed to the concrete using epoxy resin after the surface had been cleaned with air to get rid of dust. The steps for bonding the fabric to the concrete surface are as follows: First, the concrete surfaces are coated with an even layer of adhesive to ensure the surface is fully covered. The fabric, cut to the right size, is then applied to the wet resin using a flexible roller. This ensures the adhesive soaks into the fabric, and the fabric sticks firmly to the resin without folding or stretching too much (Fig. 11b). A second layer of adhesive is applied over the fabric to create a smooth, uniform bond. The second layer is applied gently with a trowel, without pressing too hard or moving in the direction of the fibers. The process is repeated for a third layer of fabric, which is added on top of the still-wet adhesive.

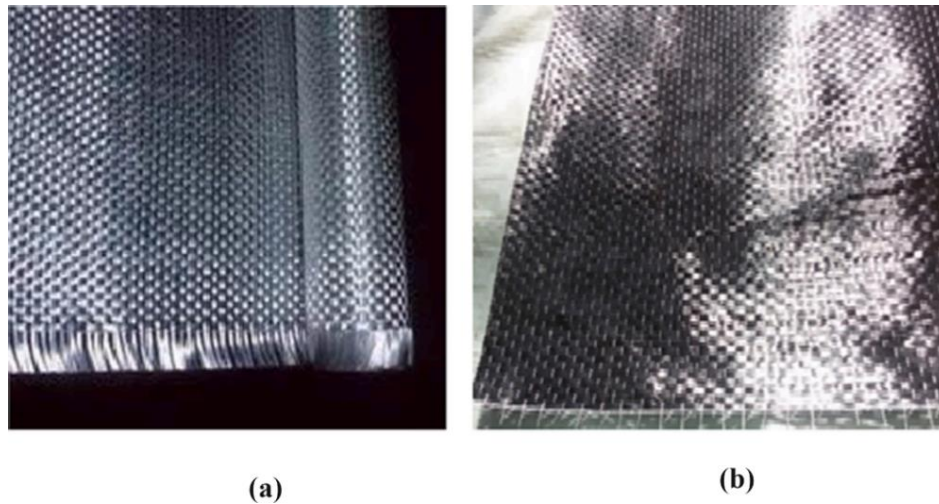


Fig. 10. Polymer fiber fabrics: a) GFRP and b) CFRP. Adapted from Karimipour et al. (2021)[7].

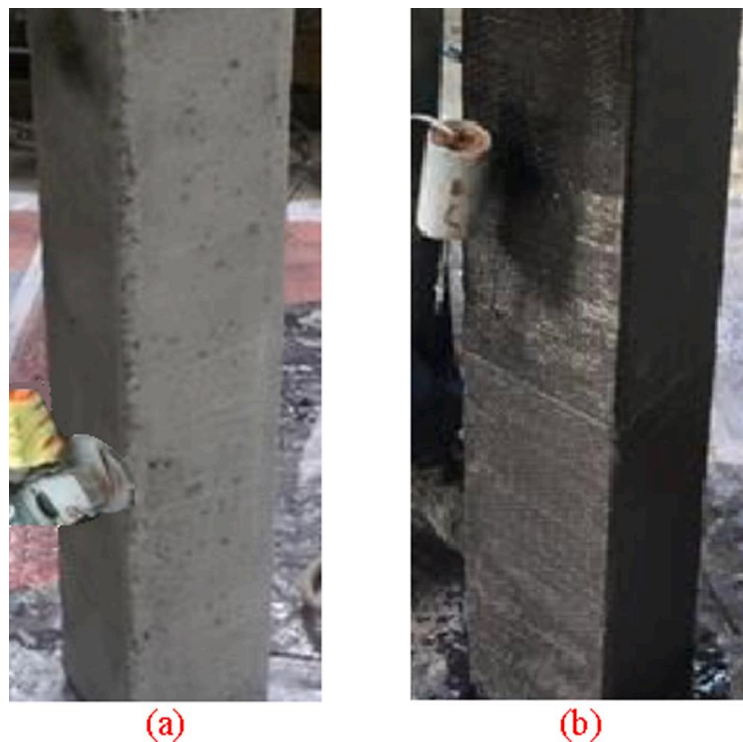


Fig. 11. Application of fabrics on the specimen surfaces. Adapted from Karimipour et al. (2021)[7].

3.1.7. Yang et al.(2021)[43]: FRP-strengthening method

Fig.12 shows the application of FRP composites on damaged concrete beams utilized in this study. After the accelerated corrosion phase, six damaged beam specimens in groups DG and DC were strengthened with FRP (Fiber Reinforced Polymer) composites. The strengthening process included three main steps: 1) preparing the concrete surfaces and corners, 2) bonding GFRP laminates or CFRP plates to the underside of the beams for added strength, and 3) installing CFRP U-jackets for extra support. In accordance with EN1504-10 [43] regulations, the concrete surfaces were roughened and the edges rounded. To close any gaps and keep air from becoming trapped during the subsequent bonding stage, a thin layer of epoxy primer (StoPox 452 EP) was sprayed after cleaning. In group DG, the wet layup process was used to apply GFRP laminates on the bottom of the beams. To create a laminate, nine layers of E-glass fiber cloth were soaked in epoxy resin (StoPox LH) and then stacked. The cloth was cut into strips that were 1500 mm long and 150 mm broad. Of the fibers, 32% ran across the beam and 68% ran along its length, using a two-part epoxy glue, a CFRP plate that was 1.5 meters long was attached to the underside of the beams. The CFRP plate

measured 100 mm by 1.45 mm and was composed of unidirectional carbon fibers (StoFRP Plate IM 100C). Both groups DG and DC received U-jackets following a 48-hour curing period. The carbon fiber fabric used to make these jackets was soaked in epoxy resin and then bonded using the wet layup method. The U-jackets positioned at a 45-degree angle were covered with three layers of cloth, while the vertical U-jackets were covered with one layer. Before the beams were evaluated for structural failure, the entire FRP system was allowed to cure for at least four weeks, with a minimum of seven days.

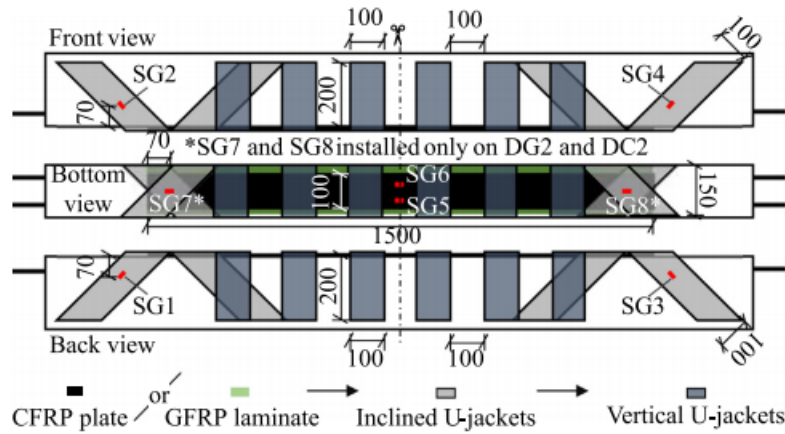


Fig. 12. Diagram showing the application of FRP composites on damaged concrete beams in groups DG and DC, along with the locations of strain gauges (SG1-SG8). Adapted from Yang et al. (2021)[43].

3.1.8. Daneshvar et al. (2021) [11]: scheme for strengthening by fiber reinforced polymer (FRP)

CFRP sheets attached to the bottom of the slabs can make the RC slabs stronger as long as the materials last. The strengthening method is shown in Fig. 13 which is utilized in this study, where CS15 and CS30 slabs were reinforced with one CFRP sheet covering the whole bottom surface and three U-shaped CFRP strips to prevent the CFRP from coming off at the ends. The CFRP sheets are 500 mm wide and cover the entire bottom of the slab. The edges of the slab were rounded to a 25 mm radius to help apply the sheets.

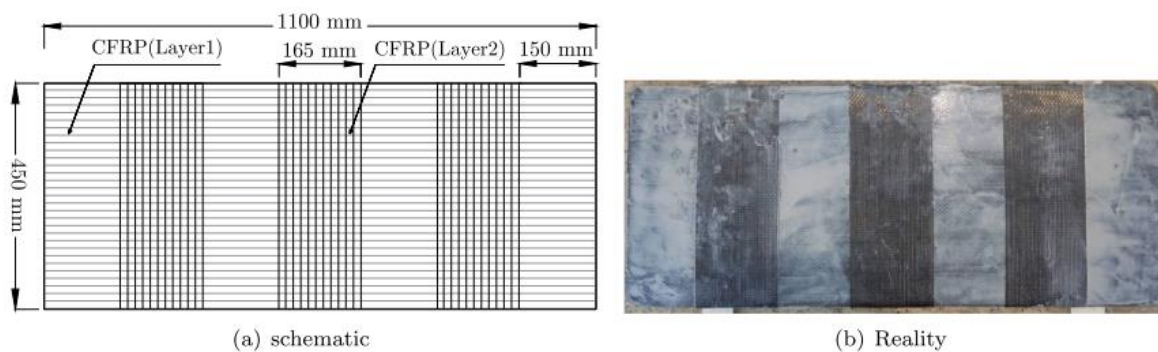


Fig. 13. Strengthening of CS15 and CS30 slabs: (a) layout and dimensions, (b) CFRP sheets applied to CS15. Adapted from Daneshvar et al. (2021)[11].

3.1.9. Al-Mashgari et al. (2021) [1]: CFRP rods and anchor bolt strengthening

Proposed repairing approach for damaged RC beam- Fig. 14 indicates, a steel plate of 110 mm in length, 90 mm in breadth, and 16 mm in thickness was used to attach the CFRP rods to the surface of the RC beam utilized in this investigation. The CFRP rods, each with a diameter of 12 mm and 2000 mm in length, were positioned along the tension area of the beams. As seen in Fig. 15, these rods were fastened to the concrete beams with two steel plates. Each plate was connected to the beam with four 8 mm anchor bolts. The RC beam's tension area was then covered with a 30 mm concrete jacketing. The two steel plates were separated

by 1750 mm. This setup ensured a strong composite bond between the concrete and CFRP rods, as the anchor bolts provide a secure connection, preventing the steel plates from detaching.

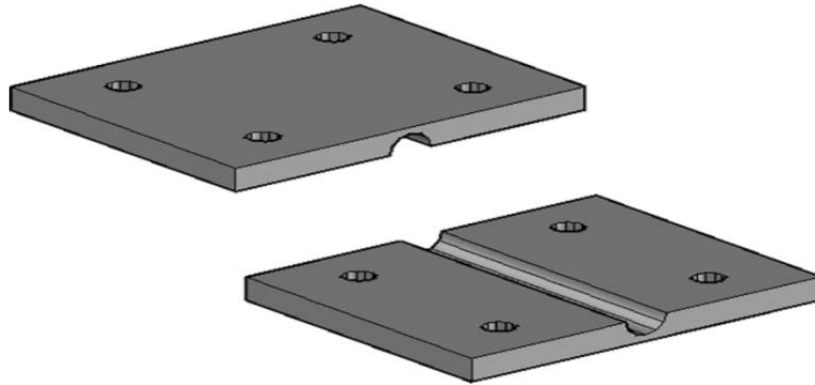


Fig. 14. Steel plate. Reproduced with permission from Al-Mashgari et al. (2021) [1].

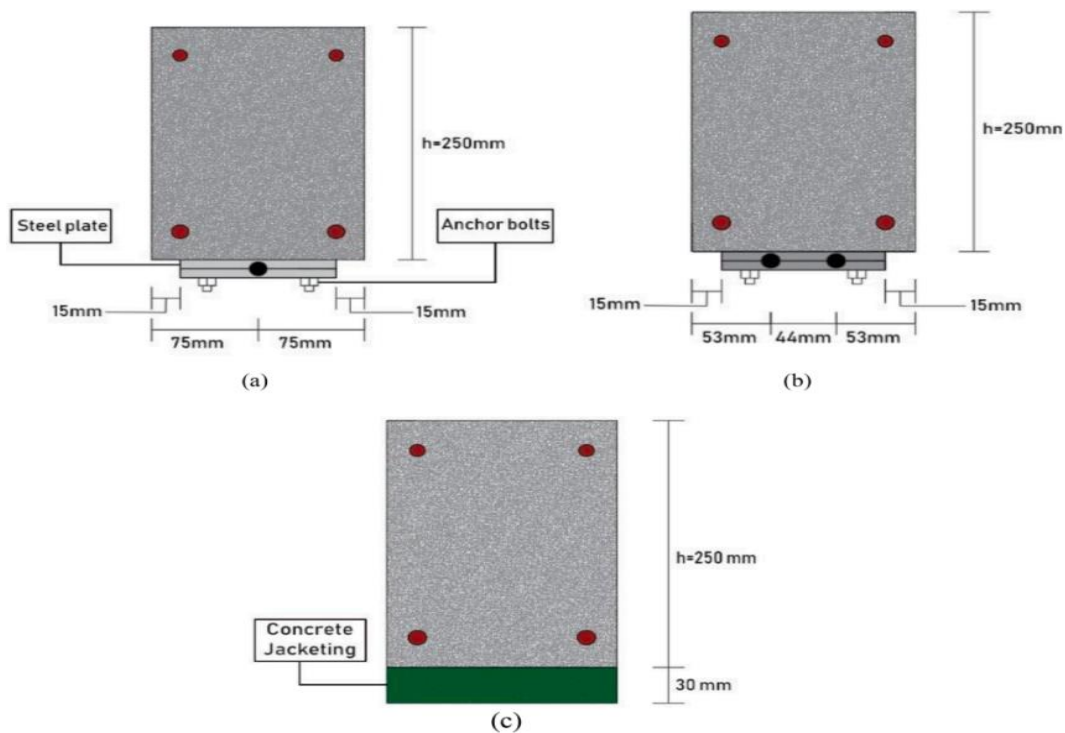


Fig. 15. Suggested Retrofitting Method: (a) Single CFRP, (b) Double CFRP, (c) Concrete Jacketing. Reproduced with permission from Al-Mashgari et al. (2021)[1].

3.1.10. Hosseini et al. (2016) [15]: near surface mounted- carbon fibre reinforced polymers (NSM-CFRP) strengthening

Application of the NSM CFRP laminates To apply CFRP laminates using the NSM method, the following steps were carried out: 1. Slits of about 5 mm wide and 25 mm deep were cut into the concrete using a diamond cutter, following the layout for the laminates. 2. The slits were cleaned with compressed air. 3. The laminates were cut to the required length and cleaned with acetone. 4. Epoxy adhesive was prepared according to the supplier's instructions. 5. The slits were filled with adhesive. 6. A layer of adhesive was applied to the laminates. 7. The laminates were placed into the slits, and any extra adhesive was removed. [58] Fig16 shows the device used to apply pressure to the laminates, which includes a system for controlling the oil pressure, hydraulic jacks to transfer force to the laminates, and load cells to measure the prestressing force utilized in this study. To ensure both ends of the RC slabs release the prestress at the same time, two steel rollers were placed under the slabs. As seen in Fig. 16, the CFRP laminates were inserted into the slits, passed through the hydraulic jacks, and secured at both ends with an active and passive anchor

once the slab had been positioned in the prestressing system. Every laminate was positioned as near to the outside of the slab as feasible. The laminate was subjected to prestressing loads, which were 20% and 40% of the laminate's ultimate tensile strength, respectively, for slabs S2L-20 and S2L-40. Steel anchors were used to secure the other end to the main frame (passive anchor), while a hydraulic jack applied force to the other end (active anchor). The prestressing load was increased at a rate of 0.5 kN/min. Once the full prestressing load was applied, the slits were filled with epoxy adhesive using a spatula (Fig. 16). Special care was taken to avoid air pockets between the concrete, adhesive, and CFRP. After about six days, the prestressing load was slowly released at a rate of 0.3 kN/min.

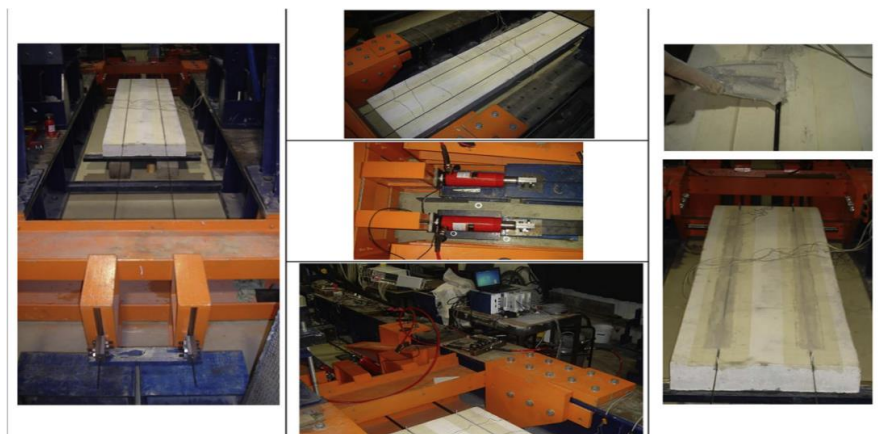


Fig. 16. Process of applying prestress to the NSM CFRP laminates. Reproduced with permission from Hosseini et al. (2016) [15].

3.1.11. Xu et al. (2020) [5]: strengthening technique using CFRP strips

Fig. 17. demonstrates the specimens' measurements and the strengthening method used in this investigation. Some corroded specimens were strengthened using a CFRP strip, which was created by applying epoxy resin to the column surface and connecting a carbon fiber sheet to it. Shanghai Hangshuo Composite Materials Co. provided the epoxy resin and carbon fiber sheet. Ltd. According to the manufacturer's data, the carbon fiber sheet had an areal weight of 293 g/cm², an elastic modulus of 214 GPa, and a tensile strength of 3113 MPa. The epoxy resin had an elastic modulus of 2672 MPa and a tensile strength of 42 MPa. The elastic modulus and tensile strength of the CFRP formed were tested according to ASTM D3039, showing values of 279 GPa and 3537 MPa, respectively.

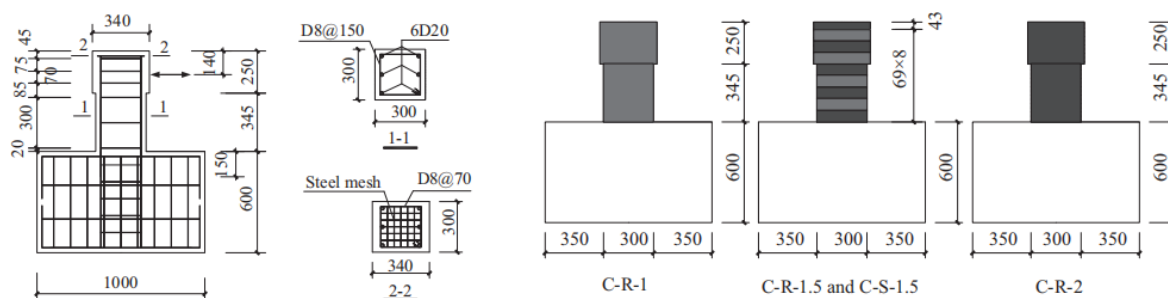


Fig. 17. Dimensions of the specimens and the strengthening technique (unit: mm). Reproduced with permission from Xu et al. (2020) [5].

3.1.12. Chotickai et al. (2021)[12]: CFRP composite strengthening

In this work, a Carbon fiber reinforced polymer (CFRP) wet-layup technique was used to strengthen steel bars with weight losses of 0%, 10%, and 20%. The specimens' corners were rounded to a radius of 25 mm. To guarantee a solid binding between the CFRP and concrete, loose objects, dirt, and voids were removed from the surface. Both contact-critical applications (such as confining columns) and bond-critical

applications (such as reinforcing beams and slabs) require this procedure. Abrasive blasting, water blasting, and bush-hammering are surface preparation techniques that roughen the concrete surface to increase bond strength [34]. Deep bush pounding, however, has the potential to weaken bonds and harm high-strength concrete [44]. Cutting grooves on the surface, filling them with epoxy resin, and then covering them with CFRP is another technique called grooving. Bond strength has been demonstrated to be enhanced by this [54], although performance is influenced by the groove's depth; shallow grooves strengthen bonds, while deep grooves weaken them [45,46].

In this investigation [47], the surface was cleaned, voids were filled with epoxy cement, and loose materials were ground away. Epoxy was not pumped into the cracks. To improve the bond between CFRP and concrete, primer was used. The CFRP fibers were bonded together using a saturating resin. The tensile strengths of the CFRP sheets and epoxy glue were 3.79 GPa and 72.4 MPa, respectively (Table 1). One layer of CFRP was applied to specimens with 0% and 10% corrosion, while two layers were applied to specimens with 20% corrosion (Table 2). ES was assigned to specimens with and without CFRP jackets. Specimens with and without CFRP jackets were labeled as ES and E, respectively, with corrosion levels noted as 0, 10, and 20. The passive confining pressure from the CFRP jacket depends on its elasticity, volumetric ratio, and the lateral strain of the concrete. For rectangular columns, the volumetric CFRP ratio (q_f) is calculated using the formula: $q_f = 2n_f t_f (b + h) / (bh)$. Here, n_f is the number of CFRP layers, t_f is the sheet thickness, and b and h are the dimensions of the rectangular concrete section. The CFRP ratios for specimens with one and two layers were 0.78% and 1.56%, respectively.

Table 1. Mechanical Properties of CFRP and adhesive. Adapted from Chotickai et al. (2021)[12].

	CFRP Sheet (0.127mm thickness)	Epoxy adhesive
Modulus of Elasticity	230 GPa	3.18GPa
Tensile Strength	3.79 GPa	72.4GPa
Tensile Strain	1.7%	5%

Table 2. Specimen details. Adapted from Chotickai et al. (2021) [12].

Specimen	Wt. Loss for Longitudinal bars(%)	Number of CFRP Layers	$\rho_f(\%)$	Number of Specimens
E0	0	0	0	2
ES0	0	1	0.78	2
E10	10	0	0	2
ES10	10	1	0.78	2
E20	20	0	0	2
ES20	20	2	1.56	2

3.2. Cementitious composite-based techniques

3.2.1. Li et al. (2023) [48]: scheme for strengthening FRECC composites

The procedures for applying the FRECC strengthening system to concrete columns are depicted in Fig. 18 of this study. This is how the procedure proceeded: (a) An electric drill was used to remove the concrete cover until it reached the reinforcements. An air compressor was then used to clean the surface (Fig. 18a). (b) To smooth the column surface, a thin layer of ECC, 3–10 mm thick, was applied. (c) After that, basalt fiber was gently pressed into the ECC layer after being wrapped around the column. (d) To fully encase the basalt fiber, an additional layer of ECC was applied. (e) As seen in Fig. 18b, this procedure was repeated using additional basalt fiber layers, making sure that each layer overlapped by 250 mm. (f) Lastly, a PVC mold (Fig. 18c) with a diameter of 192 mm to match the size of the original column was used to maintain the overall thickness of the strengthening system at 25mm.

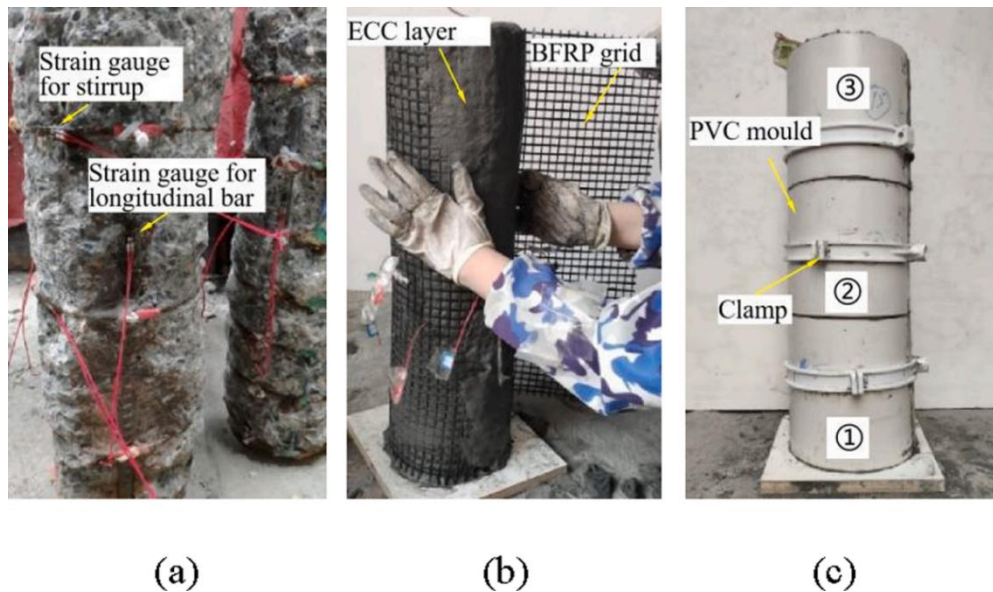


Fig. 18. Process of strengthening corroded columns using FRECC composites: (a) removal of concrete cover damaged by corrosion; (b) application of basalt fibre and ECC; (c) use of a PVC mould to control the thickness of the strengthening system. Adapted from Li et al. (2023)[48].

3.2.2. Al-Huri et al.(2023)[16]: strengthening of the corroded RC beams using ultra-high performance concrete (UHPC)

In this investigation, sandblasting was used to clean the side surfaces of the corroded specimens down to a depth of 2.5 mm after the RC beams had corroded to the appropriate levels. In order to simulate concrete spalling brought on by reinforcing corrosion, the cracked cover was then chipped away with a steel hammer. The rusted bars were scrubbed with steel brushes and dry compressed air to remove rust and any last bits of loose concrete. The strengthening arrangements of the corroded beams with different UHPC layer thicknesses are shown in Fig. 20. It is crucial to remember that the midpoint of the stirrups is used to measure the thickness of the UHPC layers applied to the specimens' bottom surfaces. To guarantee the highest compressive strength of the UHPC layers, the beam specimens were maintained damp with burlap sheets for 28 days after the UHPC was cast.

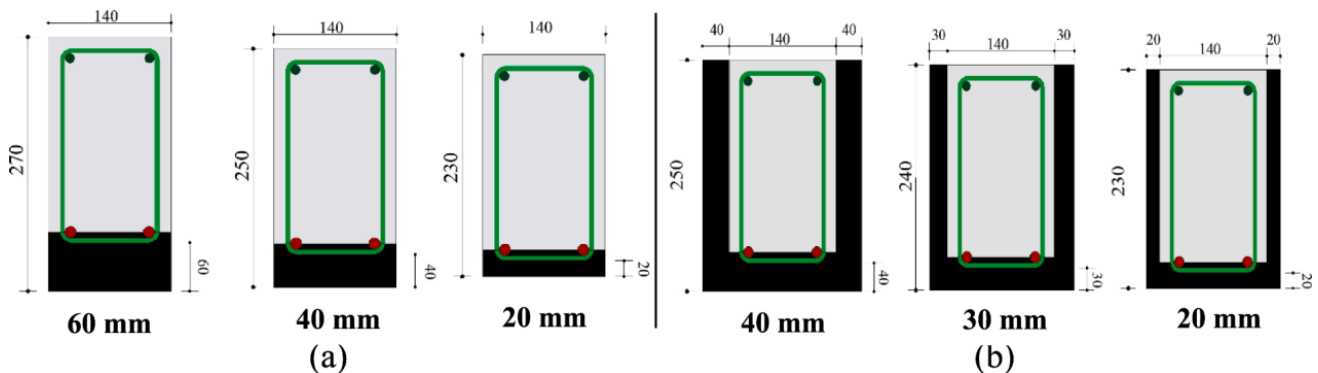


Fig. 20. UHPC layer configurations and thicknesses for strengthening corroded beams: (a) 1-sided; and (b) 3-sided (unit: mm). Adapted from Al-Huri et al.(2023)[16].

3.2.3. Feng et al. (2021)[24]: cementitious fiber reinforced composite material (C-FRCM) system

The strengthening method used in this work for corroded circular RC columns is depicted in Fig. 21. Since this region is most susceptible to damage during powerful earthquakes, the Cementitious Fiber Reinforced Composite Material (C-FRCM) system is used to reinforce the portion from the base up to 600 mm above it [49]. For circular RC columns, it is advised that the strengthening length be at least 1.2 times the diameter of the column [50]. The four stages of the CF mesh application process are shown in Fig. 22: (a) Use a

grinder to first roughen the surface of the area that needs strengthening in order to reveal the coarse aggregates. Then, use steel brushes and water to clean and wash the area. (b) To get ready for bonding with the cementitious layer, wrap the area with a sponge and completely wet it. Let it sit wet for 12 hours. (c) Cover the concrete surface with a layer of cementitious matrix. Next, firmly wrap a layer of CF mesh around the reinforced region [51]. Finally, apply another layer of cementitious matrix. To add another layer of CF mesh, repeat these steps. (d) Lastly, to stop water loss, cover the reinforced area with a protective film. After the cementitious matrix has solidified, remove the film. The cementitious matrix is 5 mm thick in each layer.

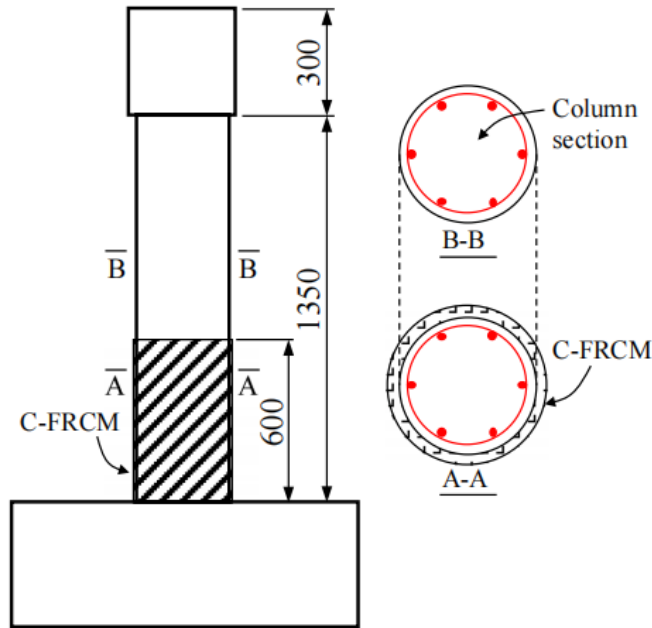


Fig. 21. Strengthening of corroded circular RC columns. Adapted from Feng et al. (2021)[24].

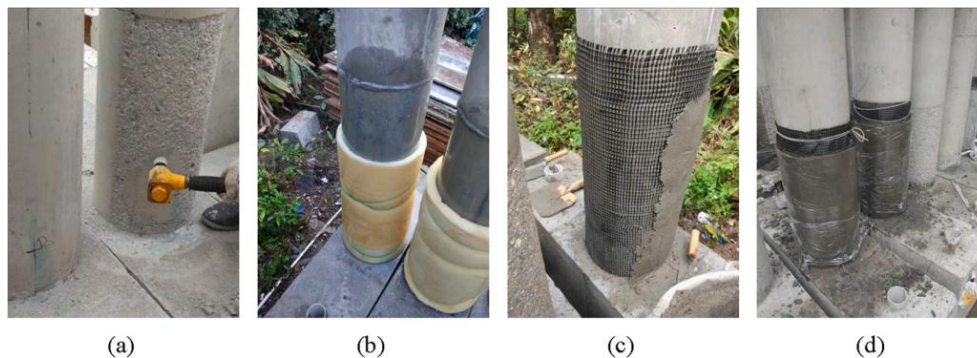


Fig. 22. Process of strengthening. Adapted from Feng et al. (2021) [24].

3.2.4. Tang et al. (2024)[52]: strengthening scheme using ultra high-performance fiber reinforced concrete (UHPFRC) jackets

Commercial normal strength concrete (NSC) from a nearby concrete plant was first used to create the RC columns. As seen in Fig. 23(a), the columns were taken out of their molds after casting and allowed to cure for 28 days in a humid atmosphere. Prior to retrofitting, each column's portions that needed strengthening were mechanically roughened to reveal the coarse aggregates. In order to improve the Ultra High-Performance Fiber Reinforced Concrete (UHPFRC) bond with the NSC, a 5-mm deep rough layer was produced. The roughened columns were soaked in water for a full day prior to casting the UHPFRC. To enable the UHPFRC to completely set, the retrofitted columns (Fig. 23(c)) were submerged in water for an additional 28 days following the casting of the UHPFRC. Every step of the planning and finishing process is displayed in Fig. 23.

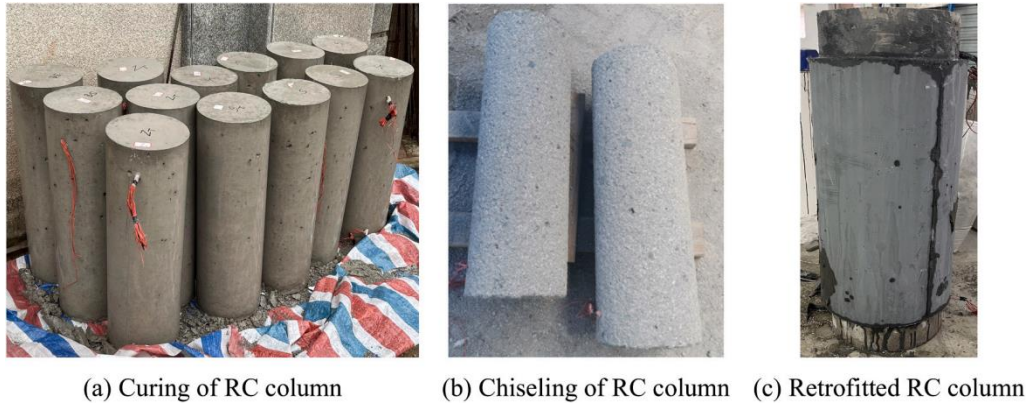


Fig. 23. Steps for preparation and retrofitting. Adapted from Tang et al. (2024)[52].

3.2.5. Zhang et al. (2023)[6]: mechanism of ECC-FRP reinforcement technology

The Von Mises stress is displayed in Fig. 24 at four critical places in the typical model FE-S0-L0-F2-A: the longitudinal steel bar with the stirrup features used in this investigation, the concrete, the ECC, and the BFRP grid. The middle portion of the ECC undergoes greater compressive stress than the sides prior to the stirrup yielding. The combined effect of circumferential tensile tension and vertical compressive stress causes the compression capacity in the center of the ECC to drop after the stirrup yields. At Point B, the concrete's compressive stress reaches 42–57 MPa, which is quite uniform. This shows that the concrete receives steady lateral support from the ECC-FRP reinforcement system. When localized buckling of the longitudinal steel bar begins, the stress decreases first in the middle of the bar after it reaches its yield strength, then spreads outwards. Point C is where the middle stirrups reach their yield stress. With maximum stresses of 11 MPa, 30 MPa, 67 MPa, and 263 MPa at Points A, B, C, and D, respectively, the BFRP grid is most stressed near the center of the column. To further explain the role of the BFRP grids, Fig. 25 shows the stresses for one and three layers of BFRP grids. It can be seen that the stress in the column with different BFRP layers is almost the same at different points. As the number of BFRP layers increases, the lateral support provided by the BFRP grids to the concrete improves during the softening stage. This helps delay the brittle failure of the strengthened column. However, the BFRP grid does not fully perform, with stresses at Points B, C, and D being only 5%, 10%, and 40% of the peak stress.

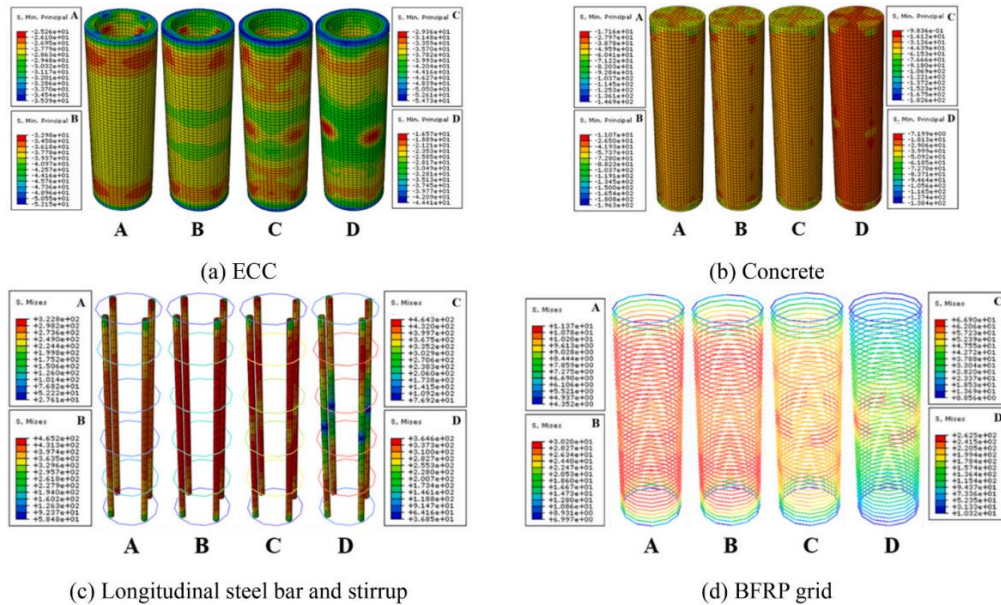


Fig. 24. Von Mises stress for the typical model. Adapted from Zhang et al. (2023) [6].

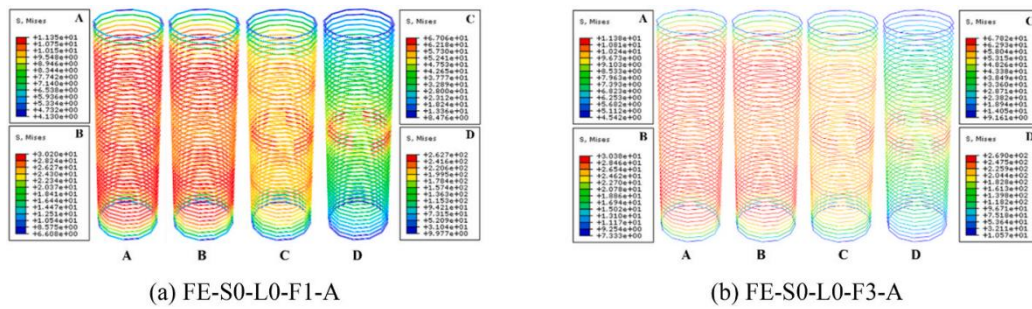


Fig. 25. Von Mises stress of the BFRP grid. Adapted from Zhang et al. (2023)[6].

3.3. Hybrid systems and electrochemical integration

3.3.1. Feng et al. (2022)[22]: impressed current cathodic protection-structural strengthening (ICCP-SS) technique

Although the traditional strengthening techniques like FRP systems and concrete jacketing were found to be encouraging, they can fall short in overcoming problems concerning long-term corrosion protection. To address these shortcomings, further advanced solutions like ICCP systems and hybrid methods have been investigated. Since the bottom of the column is typically affected by seismic stresses, Cementitious Fiber Reinforced Composite Material (C-FRCM) composites were used in this work from the base up to 600 mm in height (Fig. 27). There were three primary steps in the strengthening process: 1. Covering the concrete surface with a cement-based substance. 2. Covering the cement-based substance with a mesh of carbon cloth. 3. Adding more cement-based material to cover the carbon mesh.

To guarantee a strong bond, the concrete surface was made rough and completely wetted before work began. There were no air bubbles when the carbon cloth mesh was firmly wrapped and pressed into the cement. The ICCP (Impressed Current Cathodic Protection) technology was used after the columns had been corroded for 180 days using an expedited procedure. The carbon fabric mesh was linked to the positive terminal of a DC power source, and the steel bars at the top of the column were connected to the negative terminal, as seen in Fig. 26. By concentrating oxidation reactions at the anode (carbon mesh), this configuration stopped the steel bars from corroding. Columns lacking Cementitious Fiber Reinforced Composite Material (C-FRCM) composites, such as L0-N3-C360-P20 and L0-N6-C360-P20, were anoded by wrapping carbon fabric mesh around the column. While oxygen was oxidized at the cathode (steel bars), corrosion was avoided. The evolution of chlorine took place at the anode (carbon mesh). Prior to cyclic loading experiments, the ICCP system was run for 180 days at a current density of 20 mA/m². All specimens were continuously exposed to dry-wet conditions during this time. The steel re-bars potential was measured using external devices and a saturated copper sulfate reference electrode at 25°C as depicted in Fig. 28.

According to BS EN ISO 12696:2016 standards [50], the steel potential should not go more negative than -1100 mV (relative to Ag/AgCl/0.5 M KCl). ICCP effectiveness was checked based on three criteria:

- VOFF \leq -720 mV relative to Ag/AgCl/0.5 M KCl.
- Steel potential after 24 hours \geq VOFF + 100 mV.
- Steel potential after 24 hours \geq VOFF + 150 mV when reference electrodes were used for more than 24 hours. VOFF refers to the "Instantaneous OFF" potential of steel. During ICCP protection (shown in Fig. 29), steel potential was recorded at three moments. "Instantaneous OFF" (red dashed lines), 2.4 hours after "Instantaneous OFF" (blue dashed-dot lines), 3.24 hours after "Instantaneous OFF" (black solid lines). Threshold values of -1100 mV and -720 mV were also marked in the figure. For all specimens, the potential at "Instantaneous OFF" was above -1100 mV, and some exceeded -720 mV during the protection period. Additionally, the potential change before and after 24 hours was greater than 150 mV in all specimens. This confirms that the ICCP system meets current code requirements for protecting steel in concrete through cathodic protection.

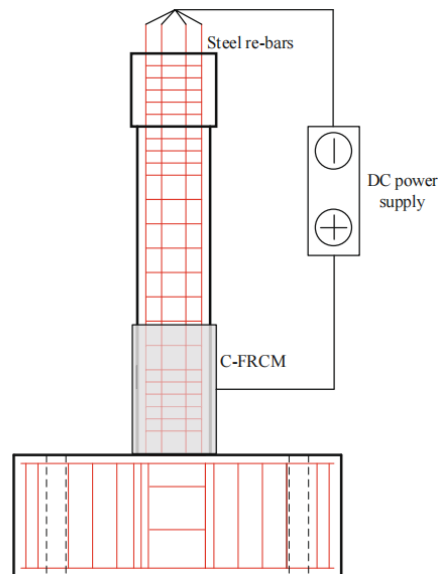


Fig. 26. illustrates a schematic diagram of the ICCP (Impressed Current Cathodic Protection) system. Adapted from Feng et al. (2022) [22].

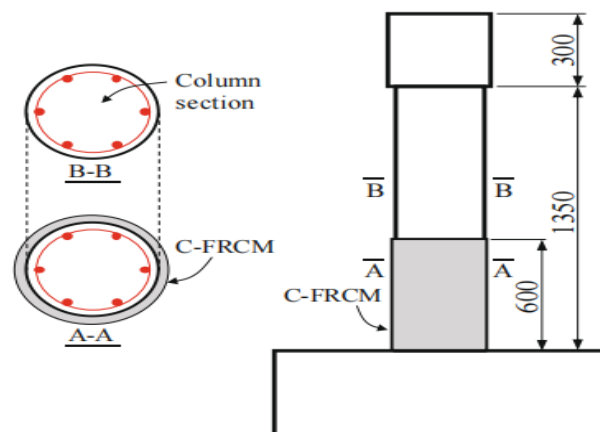


Fig. 27. shows the method used to strengthen corroded circular reinforced concrete (RC) columns. Adapted from Feng et al. (2022) [22].

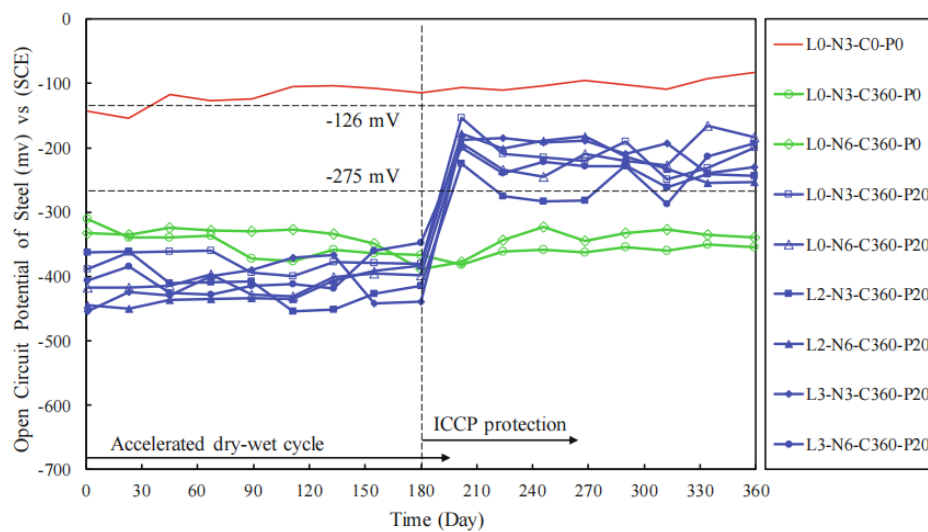


Fig. 28. displays the open circuit potential measurements of the steel re-bars.

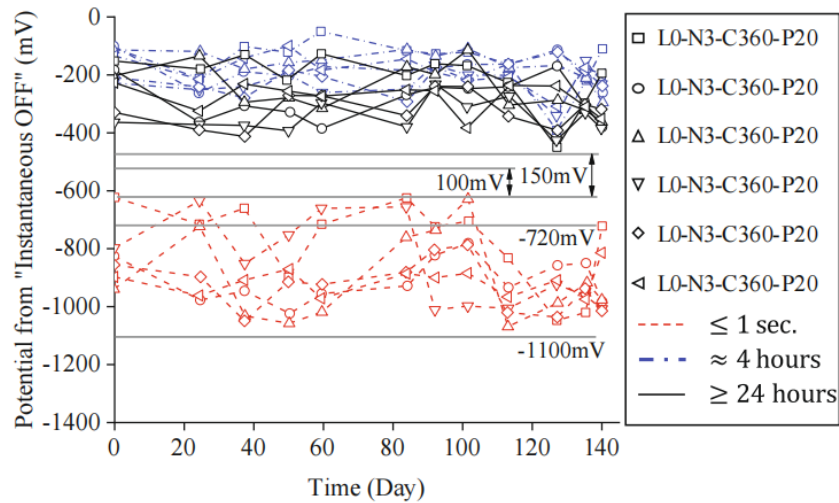


Fig. 29. presents the potential of reinforcing steel recorded from the "Instantaneous OFF" state. Adapted from Feng et al. (2022) [22].

3.3.2. Panuwat et al. (2024)[53]: construction of ferrocement and FRP composites strengthening process

Steel cages were positioned inside the timber formworks used to cast each slab. Concrete was compressed using mechanical vibrators before being put into the formworks. Fig. 30., used in this study, depicts a typical construction process. Two different kinds of anchors were used in this investigation. Drilling holes in the slabs, thoroughly cleaning them, and then putting the golden portion of the anchor (shown in Fig. 31(a)) into the holes was the process of installing mechanical anchors. Figure 33(a) illustrates how the slabs are strengthened with FRP jackets. Hand rollers were used to apply epoxy to the slabs' surface before FRP layers soaked in epoxy were added. The load was distributed uniformly over the steel plates across the slabs, as shown in Fig. 33(c). After the FRP layers were applied, holes were drilled through them, chemical anchors were installed in these holes, and steel plates were added. Finally, nuts and washers were used to complete the strengthening process.

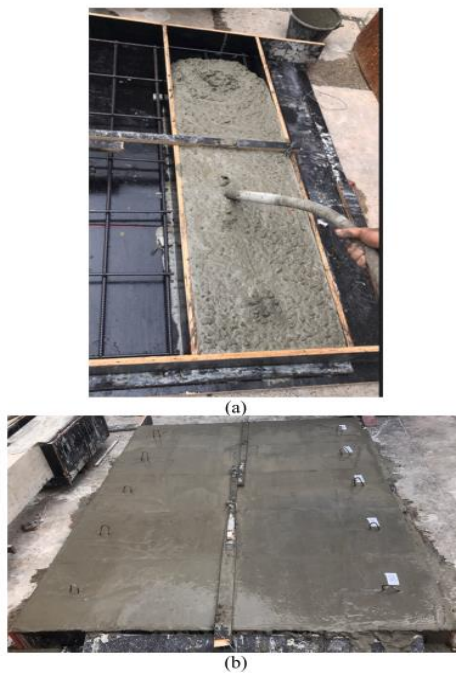


Fig. 30. Slab construction process: (a) concrete being poured and compacted, and (b) slabs prepared for curing. Adapted from Panuwat et al. (2024)[53].

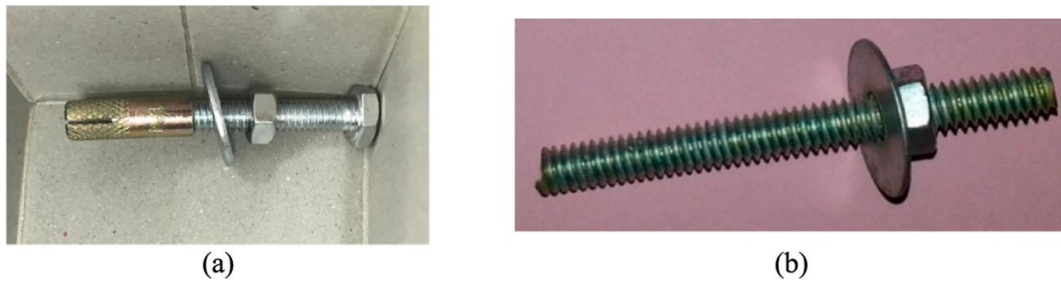


Fig. 31. Common types of anchors: (a) mechanical and (b) epoxy-based (chemical).Adapted from Panuwat et al. (2024) [53].

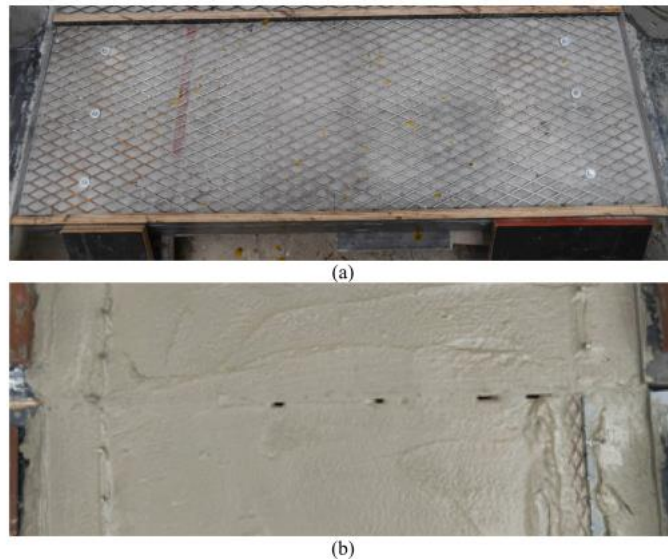


Fig. 32. Slab strengthened with mechanical anchors: (a) wire mesh and mechanical anchor installation, and (b) plastering finished to complete the ferrocement jacket.Adapted from Panuwat et al. (2024)[53].



Fig. 33. Installing FRP layers with chemical anchors: (a) applying epoxy, (b) bonding CFRP to the concrete surface, and (c) placing threaded rods into concentric holes in steel plates and slabs.Adapted from Panuwat et al. (2024) [53].

3.3.3. Zheng et al. (2019)[19]: CFL and steel plates technique

The following procedures were used to get the slabs ready for bonding the reinforcing materials after 28 days. First, at the designated places, anchor bolt holes (8 mm in diameter and 80 mm in depth) were drilled (Fig. 34). Then, the surface was polished using a grinding machine to remove the weak top layer of concrete (approximately 1 mm thick) until the aggregates were exposed. Next, the strengthening materials were prepared. The carbon fiber laminate (CFL) was pre-saturated and made from T700-12 k carbon fibers, and the steel plates were cleaned using a steel brush to remove rust. Holes were drilled in the steel plates to match the ones in the slab, and the bonding surface was roughened and cleaned with acetone. The CFL and steel plates were then cut to the required lengths. Before bonding, the slab and holes were cleaned using high-pressure air, and acetone was applied to the concrete surface. The epoxy adhesive was mixed according to the instructions and spread evenly on the bonding surface. The CFL was carefully laid down, ensuring it was smooth and the fibers were straight. A plastic scraper was used to press the CFL to remove air between the slab and CFL. To improve anchorage, epoxy adhesive was injected into the cleaned holes, and bolts were inserted. The CFL or steel plates were bonded at the correct locations, with the fibers bypassing the bolts without damage. When the CFL and steel plates overlapped in the D1 and D2 groups, epoxy adhesive was applied to the inner layer, allowed to set, and then the outside layer was added (Fig 35). Prior to testing, the slabs were cured in the lab for more than a week after bonding.

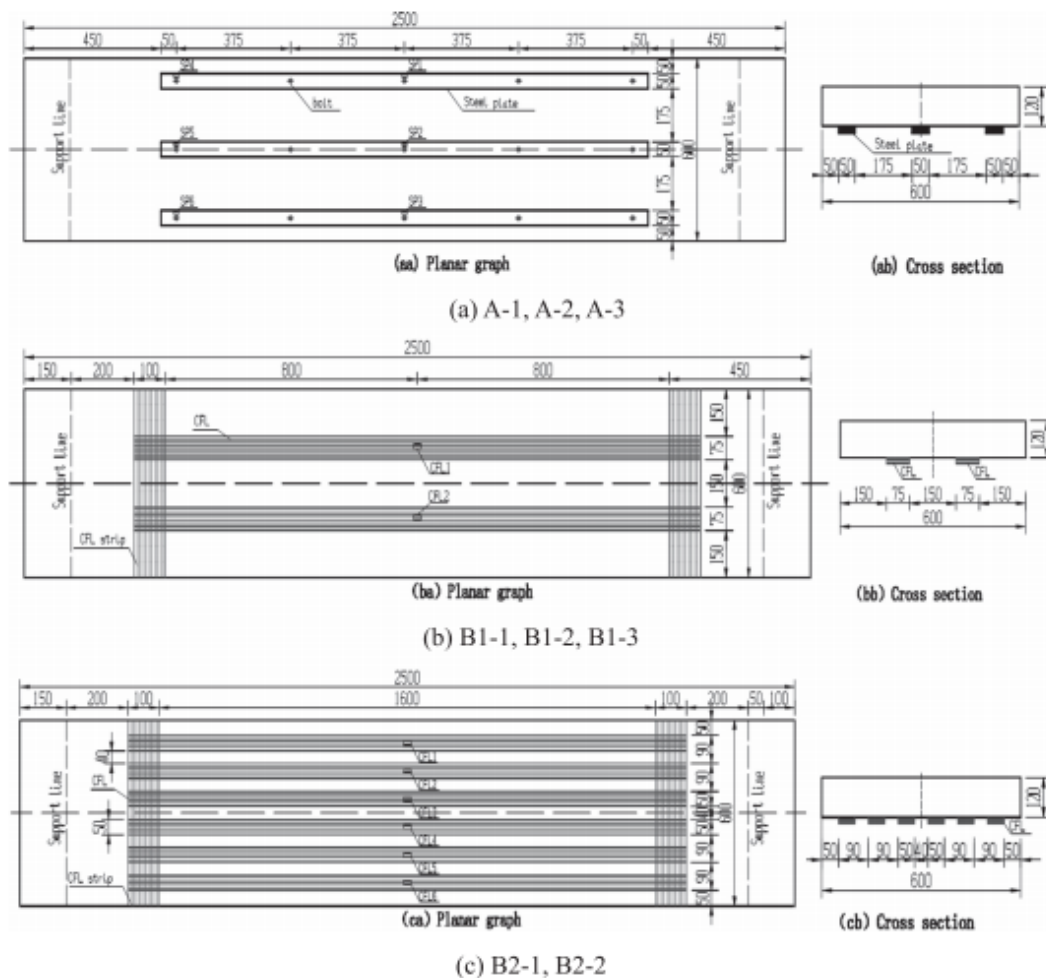


Fig. 34. Details of the strengthening process and positions of strain gauges (units: mm) (steel bolt, strain gauges for CFL labeled CFL1 to CFL6, and strain gauges for steel plates labeled SP1 to SP6). Adapted from Zheng et al. (2019)[19].

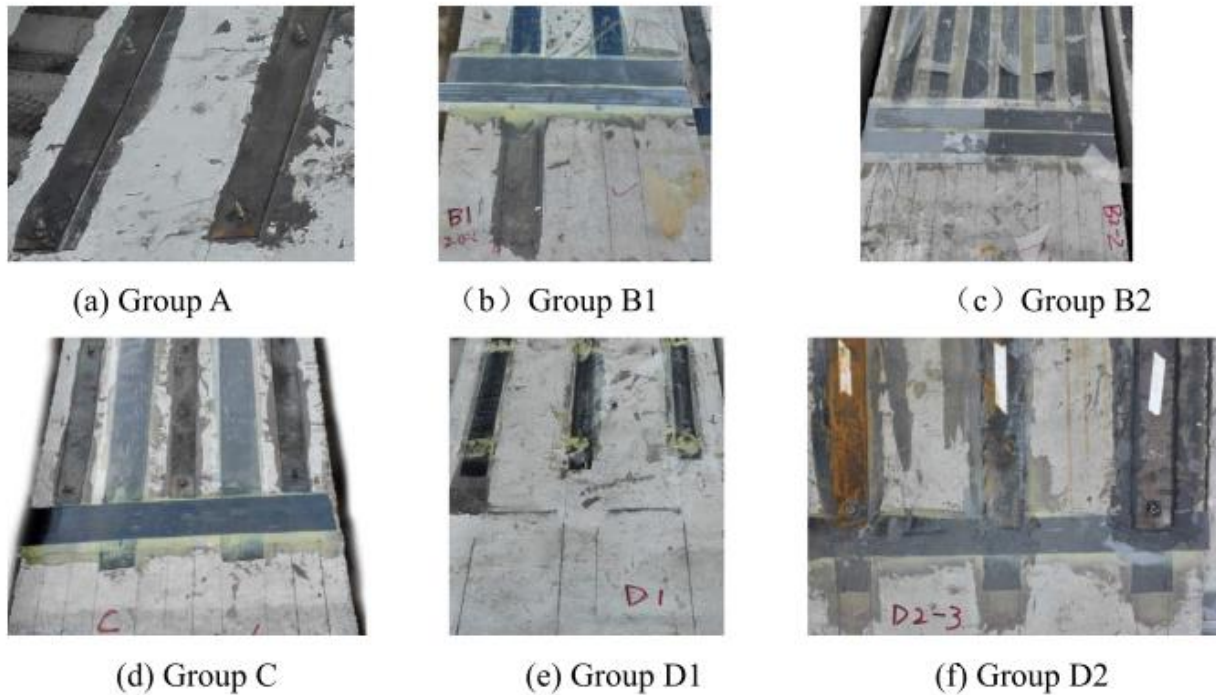


Fig. 35. Various types of anchors at the ends of the strengthened slabs. Adapted from Zheng et al. (2019) [19].

3.4. Textile-based strengthening

3.4.1. Fang et al. (2021) [54]: basalt fibre textile strengthening (BFRP or BTRM) scheme

As seen in Figure 36, reinforcing materials (BFRP or BTRM) were put to the bottom of the corroded RC slabs over a 2000 mm area during the test in this investigation. No particular anchoring treatment was applied at the ends, and the strengthening materials did not extend to the support area. By altering variables such as the starting corrosion level, the strengthening materials (BFRP or BTRM), and the quantity of basalt textile layers, the test sought to examine the flexural performance. The specimens' details are displayed in Table 3. Moderate or severe corrosion is indicated by the first letter of the specimen name (M or S). The type of strengthening is indicated by the second letter, where (C) denotes no strengthening and (P or M) denotes strengthening with BFRP or BTRM respectively. Three or five layers of textile are represented by the last two numbers, respectively. For instance, "M-P-30" denotes a slab that has moderate corrosion and has been reinforced with three layers of BFRP. The wet layup method was employed in the strengthening process, which included the following steps: (1) prepping the concrete surface by marking the bonding areas, using a bush hammer to roughen the surface down to a depth of approximately 3 mm, and using compressed air to remove any dust. (2) In order to reinforce BFRP, the cloth was brushed with adhesive and compressed layer by layer using a plastic roller. This was done five times to ensure the adhesive soaked effectively and to remove surplus polymer. (3) In order to reinforce BTRM, (a) water was added to the concrete surface; (a) To guarantee adequate mortar impregnation into the textile, layers of mortar and textile were applied, maintaining the overall thickness of the BTRM at 10 mm. The mortar layers that made up the first and last layers of BTRM were both 2 mm thick, and the intermediate layers for the three textile layers were likewise 2 mm thick.

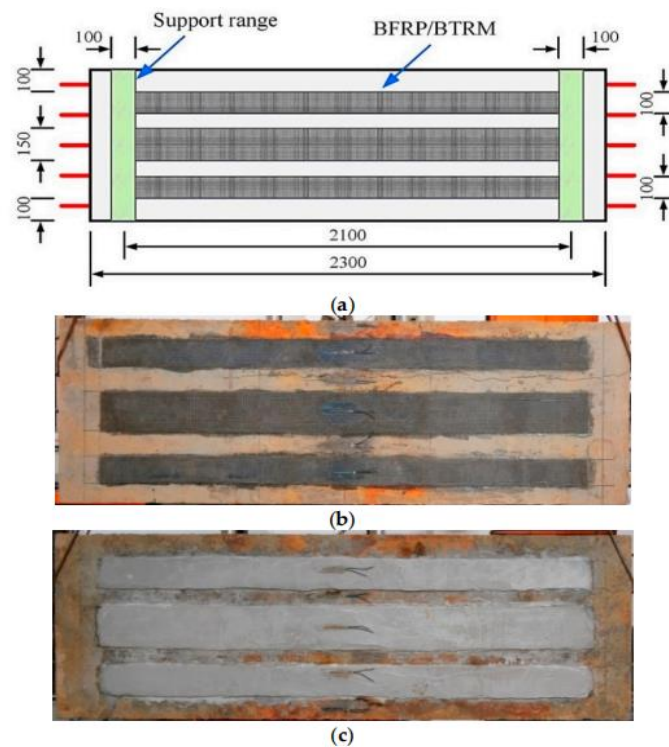


Fig. 36. Test specimen details with applied strengthening materials: (a) strengthening layout (all dimensions in mm); (b) specimen strengthened with BFRP; (c) specimen strengthened with BTRM. Adapted from Fang et al. (2021) [54].

Table 3. BTest Strengthened specimen details. Adapted from Fang et al.(2021) [54].

Specimen ID	Initial Corrosion Rate (Expected Corrosion Ratio) %	Number of Textile Layers	Strengthening Material
M-C	8	-	-
M-P-3	8	3	BFRP
M-P-5	8	5	BFRP
M-M-3	8	3	BTRM
M-M-5	8	5	BTRM
S-C	16	-	-
S-P-3	16	3	BFRP
S-P-5	16	5	BFRP
S-M-3	16	3	BTRM
S-SM-5	16	5	BTRM

4. Comparative analysis of strengthening techniques for corroded RC members

The comparative analysis of 21 RC structure strengthening techniques for corrosion-damaged structures shows clear trade-offs between improvement in load capacity, durability, cost, and simplicity of application. UHPC overlays, UHPFRC jackets, and ECC-FRP composites present very high loads and durability improvements, which are suitable for extreme corrosion conditions but tend to be very labor-intensive and expensive. Conversely, CFRP strips, CFRP/GFRP fabric, and BFRP/BTRM textile yield moderate benefits with greater ease of use and lesser expenses, being best suited for rapid or low-cost interventions. Hybrid systems such as ICCP-SS with C-FRCM and CFL anchored to steel plate exhibit sustained corrosion protection and mechanical strengthening, albeit requiring more intricate installations. Prestressed NSM-CFRP laminates and CFRP anchors are particularly noteworthy for their exceptional structural performance; however, they require precise detailing and careful setup. This contrast emphasizes that the best technique choice should reconcile structural requirements, exposure conditions, and practical limitations.

Table 4. Comparative Analysis of strengthening techniques.

Sl. No.	Strengthening Method	Load Capacity Improvement	Durability Enhancement	Cost	Ease of Implementation	Remark
1	NSM-BFRP & NSM-GFRP	High	Moderate	Moderate	Moderate	Enhanced bond using grooves; epoxy application and spacers crucial.
2	CFRP Anchors	High	High	High	Moderate	Excellent anchorage; sensitive to detailing and epoxy bonding quality.
3	FRECC Composites	High	High	High		Multi-layer ECC and basalt wrapping; ideal for columns.
4	UHPC Overlay	Very High	Very High	High	Low	Increases flexural strength and crack resistance; labour-intensive.
5	C-FRCM System	Moderate	High	Moderate	Moderate	Good for seismic regions; requires surface prep and curing.
6	CFRP Laminates (Bonded)	High	Moderate	High	High	Simple application; debonding issues possible.
7	ICCP-SS Hybrid with C-FRCM	High	Very High	Very High	Low	Prevents future corrosion and strengthens; complex setup.
8	UHPFRC Jackets	High	Very High	High	Moderate	Excellent bond with NSC; 28-day curing required.
9	CFRP-GFRP Hybrid Laminates	High	High	Moderate	Moderate	Hybrid action improves ductility and resistance to debonding.
10	ECC-FRP Composite	Very High	High	High	Low	Improved lateral support; delays brittle failure.
11	CFRP & GFRP Fabrics	Moderate	Moderate	Moderate	High	Applied using wet layup; prone to folding/stretching if not carefully applied.
12	FRP Composites with U-Jackets	High	High	Moderate	Moderate	Multi-layer U-jackets enhance confinement and flexural resistance.
13	Ferrocement + FRP Jackets	Moderate	Moderate	Low	Moderate	Uses mechanical and chemical anchors; ideal for slabs.
14	FRP for Slabs (CFRP bottom + U-wraps)	High	High	Moderate	Moderate	Simple yet effective layout; corners must be rounded.
15	BFRP/BTRM Basalt Textile	Moderate	High	Low	High	Wet layup method; improved for multiple textile layers.
16	CFRP Rods with Anchor Bolts	High	Moderate	Moderate	Moderate	Steel plate anchorage enhances performance; concrete jacketing used.
17	NSM-CFRP Laminates (Prestressed)	Very High	High	High	Low	Requires prestressing setup; precision needed to avoid air gaps.
18	CFRP Strips	Moderate	Moderate	Low	High	Fast installation; epoxy bonding critical.
19	CFRP Composite for Bars & Columns	High	Moderate	Moderate	High	One or two layers depending on corrosion level; groove depth critical.
20	ICCP-SS (Impressed Current + C-FRCM)	High	Very High	Very High	Low	Monitors steel potential; ideal for long-term corrosion control.
21	CFL + Steel Plate Anchoring	High	High	High	Moderate	Combines fiber and mechanical anchorage; uses epoxy and bolt injection.

5. Effect of investigated parameters

5.1. Ultimate load and corresponding deflection

Significant differences are found depending on the degree of corrosion and the strengthening methods used in a thorough analysis of the ultimate load and deflection behavior in corroded and strengthened concrete elements. For example, ultimate loads in beams A18, A12, A6, and A0 were reported to be 57.5, 62.2, 75.4, and 114.5 kN, respectively, indicating a decrease in load-carrying capacity as a result of corrosion. In particular, compared to its uncorroded counterpart B12, beam A12 showed a 20.6% lower deflection capacity and a 26.7% lower failure load. Similarly, stirrup corrosion caused load reductions of 40%, 25%, and 17.5% in beams B18, B12, and B6 compared to beam B0[2]. Using Carbon Fibre Reinforced Polymer (CFRP) rods to strengthen corroded beams increased ultimate load by up to 32% and deflection by up to 52%, significantly enhancing structural performance [1]. Research on FRP-reinforced slabs also revealed better deflection and impact resistance, but excessive corrosion reduced the efficacy of retrofitting [11]. While strengthened slabs demonstrated improvements of up to 62.79% in peak load and over 115% in deflection, reference slabs without strengthening recorded peak loads of 42.14 kN with ultimate deflections of 38.23 mm[53]. While prestressed CFRP reinforcement increased slab capacity by up to 134%, albeit with less deflection [15], ultra-high performance concrete (UHPC) strengthening further increased ultimate load by 23.7% and stiffness in girders [9]. On the other hand, corrosion up to 30% decreased failure displacement by 58% and ultimate strength by up to 56% [8]. Depending on the degree of corrosion and the number of layers used, Ultra High-Performance Concrete (UHPC) or Carbon Fibre Reinforced Polymers (CFRP) strengthening in beam studies increased ultimate loads by as much as 162% [27]. In a similar vein, slabs reinforced with Near Surface Mounted-Basalt Fibre Reinforced Polymers (NSM-BFRP) bars saw notable deflection control and increases in ultimate loads of 45–50% [14]. Although corrosion reduces load-bearing and deformation capacities, it is clear from numerous studies that appropriate strengthening methods, like CFRP, UHPC, and FRP systems, successfully restore or surpass initial performance metrics.

Corrosion significantly reduces the ultimate load and deflection capacity of RC members, with strength losses ranging up to 56% and displacement reductions of 58% in extreme cases. However, effective strengthening techniques such as CFRP, Ultra High-Performance Concrete (UHPC), prestressed laminates, and NSM-BFRP bars can recover or even exceed original structural behavior. Gains of 162% in ultimate load and over 115% in deflection are obtained based on strengthening configuration and the degree of corrosion. This highlights the effectiveness of high-performance strengthening systems in capacity strengthening as well as ductility.

5.2. Initial stiffness and post cracking stiffness

Numerous studies have focused on the stiffness behavior of reinforced concrete (RC) members that have been strengthened and corroded. A number of factors, such as the degree of corrosion, the strengthening method, and the material properties, influence this behavior. The initial stiffness of the tested beams varied slightly, according to [1], with beam B-02 exhibiting a notable drop that was ascribed to corrosion-induced steel degradation. However, because of the strengthening's ability to prevent cracks, repaired beams using Carbon Fibre Reinforced Polymers (CFRP) rods maintained almost their original stiffness levels. Similar results were seen in[7], where corroded RC columns rapidly lost stiffness after yielding as a result of rebar deterioration. Stiffness was effectively restored and improved by Carbon Fibre Reinforced Polymers (CFRP) and Glass Fibre Reinforced Polymers (GFRP) fabrics. Corrosion caused significant stiffness loss in slabs exposed to impact loading [11], but CFRP strengthening not only restored but also exceeded the original stiffness of intact specimens. The importance of stiffness in assessing structural integrity is further supported by studies such as [53] and [9]. emphasized the function of Ultra High-Performance Concrete (UHPC) in enhancing the flexural stiffness of hollow slab girders, particularly in the elastic-plastic

transition, whereas [53] observed slight variations in pre- and post-cracking stiffness based on the strengthening mechanism. Although light corrosion may initially increase stiffness due to improved bond conditions, other works, like [8] and [12], quantified the influence of corrosion and showed a reduction of up to 41%. Curiously, [12] also discovered that CFRP jackets could greatly increase the stiffness of severely corroded columns. Comparative data from [55], [14], and [27] showed that CFRP strengthening consistently resulted in higher initial and post-cracking stiffness, highlighting the importance of strengthening technique and ratio, particularly in multi-layer or NSM configurations. Similar improvements were reported by [54] and [18] using Textile Reinforced Mortar (TRM) and Ultra High-Performance Concrete (UHPC) jacketing, respectively. [18] documented up to 33% higher stiffness in retrofitted specimens. This is consistent with research from [52], which showed that even after cracking, Ultra High-Performance Fiber Reinforced Concrete (UHPFRC) jackets retained linear axial stiffness behavior. Overall, it is evident from the literature that corrosion severely reduces the initial and post-cracking stiffness of RC elements. However, stiffness performance can be successfully restored or even improved through targeted repair and strengthening techniques, especially when CFRP, UHPC, TRM, or hybrid systems are used.

Corrosion impacts initial and post-cracking stiffness negatively but to the tune of as much as 41%. CFRP rods, GFRP sheets, UHPFRC, and TRM systems, on the other hand, are efficient at restoring or enhancing stiffness. Multi-layer or NSM configurations exhibit uniform performance when elastic or cracked. UHPC and UHPFRC jackets particularly assist in delivering linear stiffness following cracking. These results highlight the way material and technique choice is reliant on the requirement of stiffness restoration in corroded structures.

5.3. Energy absorption for the pre and post cracking stages

In particular, corrosion and strengthening methods have been extensively studied in relation to the energy-dissipating capacity of reinforced concrete (RC) elements, which is commonly defined as the area under the load-displacement curve before failure. For the S1 and S3 series slabs, studies demonstrate that energy absorption rose with corrosion up to 20% before declining because of the decreased punching shear strength. On the other hand, as corrosion increased, the S2 series showed a steady decrease in energy absorption [3]. This pattern is in line with research from [8], which found that corrosion-induced loss of reinforcement and bond strength was the reason for a notable decrease in energy absorption of 69.5% and 70.3% for S1-30 and S2-30, respectively. Corrosion also lowers energy absorption capacity, which is important for reducing seismic forces, as [7] showed. CFRP and GFRP strengthening could significantly lessen this effect and improve energy absorption by 96% and 130%, respectively. Studies by [53] and [15] emphasized the significance of post-cracking energy absorption, pointing out that strengthening greatly improved the energy dissipation capacities at all prestress levels. Although energy consumption showed a near-linear decrease with increasing prestress [15], prestressed CFRP laminates in particular were effective in improving the energy performance of RC slabs during loading [15]. Studies like [26] went into further detail about how corrosion affects energy dissipation, particularly when it comes to changing failure modes from flexural to punching shear failure. A substantial drop in absorbed energy following the initial impact (average 29%) was found in studies conducted under impact loading [11], indicating serious damage. However, by slowing the spread of cracks and increasing ductility, ultra-high-performance concrete (UHPC) overlays [16] and Ultra High-Performance Fiber Reinforced Concrete (UHPFRC) jackets [52] enhanced energy dissipation. Even with differing degrees of corrosion, studies on slabs reinforced with near-surface mounted (NSM) bars [14] and ECC with basalt fibers [48] also demonstrated notable gains in energy absorption after cracking. Additionally, CFRP-strengthened columns subjected to cyclic loading showed energy dissipation improvements of up to 239.3%, highlighting the critical role that strengthening plays in preserving structural integrity [5].

Corrosion decreases the dissipating capacity of RC members by up to 70%, reducing seismic ductility and resilience. Strengthening techniques such as CFRP, GFRP, ECC, UHPC, and NSM significantly contribute

to energy absorption, with boosts ranging between 96% and 239%. Prestressed CFRP system and Ultra High-Performance Fiber Reinforced Concrete (UHPFRC) jackets contribute to increased post-cracking energy dissipation. Effective strengthening delays the growth of cracks, improves ductility, and rearranges failure modes into more desirable patterns, preserving structural integrity under impact or cyclic loading.

5.4. Combined effects from multi-parameter comparative analysis

Many studies analyze the impact of strengthening methods or corrosion in isolation, but various studies have identified the combined influence of interacting parameters on structural response, such as the type of loading, number of layers, severity of corrosion, and type of strengthening. When ultra-high performance concrete (UHPC) or CFRP rods overlays were used, for instance, beams with increasing levels of corrosion (A18 to A0) experienced successive reductions in load capacity; recovery was a function of layer number and quality of bond [1,9,27]. The stiffness-ductility trade-offs in performance were demonstrated by prestressing CFRP reinforcement, which increased ultimate capacity by as much as 134%, though often at the expense of less deflection [15]. Increased corrosion in slabs susceptible to impact diminished strengthening effectiveness, suggesting that corrosion degrades the bond and affects the retrofit interface [11]. With energy absorption improvements of up to 239% in CFRP-strengthened columns, multi-layer FRP design improved stiffness and energy dissipation, especially under cyclic and impact loads [5]. Similarly, UHPC jacketing has been shown to restore energy capacity and flexural stiffness even following significant deterioration [16,52]. According to these research, performance is not determined by a single factor but rather by a combination of factors that affect ultimate load, stiffness, failure mode, and energy dissipation. These factors include corrosion-induced damage, the strengthening system that is chosen, the stacking strategy, and the imposed loading circumstances. This highlights the importance of integrated design strategies tailored to specific damage states and service environments, as well as the need for holistic experimental or numerical investigations.

6. Load deflection behaviour

The load-deflection behavior of reinforced concrete components varies with corrosion levels and strengthening techniques, showing unique performance trends across diverse studies. In most cases, the curves exhibit multiple stages: an initial elastic range, followed by cracking, post-yield hardening, failure, and drops in stiffness or sharp increases in deflection, showing distinct plateaus [15,21,23,53]. A number of studies have reported that advanced stages of corrosion typically lower the pre- and post-cracking stiffness, contributing to existing cracks and diminished rebar cross-section area. Other studies demonstrate that with increasing levels of corrosion, bending resistance and energy dissipation significantly decrease, accompanied by a reduction in deflection at failure [3,8,12,22]. Notably, some slab-column connections tend to exhibit changed failure modes due to corrosion from flexural to punching shear, modifying the overall load-deflection response [3,26]. A few studies emphasize that the corrosion level coupled with the arrangement of reinforcement may influence the ductility of corroded slabs and beams. For example, the S2 series showed reduced displacement at failure, while the S1 and S3 series specimens showed increased ductility with higher corrosion because of the reduced effective reinforcement ratio [3]. CFRP-strengthened members demonstrated enhanced load-carrying capacity and maintained deflection levels in beams, whereas unstrengthened corroded specimens frequently showed abrupt drops in stiffness. Hardening behavior, linear post-yield responses, and delayed failure onset were all influenced by CFRP and BFRP materials [4, 7, 24]. In certain configurations, strengthened slabs even outperformed uncorroded control specimens in terms of ultimate capacity and early stiffness [14,16,20]. Notably, research has shown that hybrid strengthening systems, like NSM-FRP bars and the CFL-SP technique, greatly increased stiffness and ductility [14,19]. Furthermore, numerical and experimental research validates that finite element simulations accurately depict flexural behavior, including failure patterns, stiffness variations, and cracking loads [4,9,15]. At low corrosion rates, stirrup corrosion was found to have an impact on stress distribution

without significantly changing load-deflection trends [2]. Last but not least, it has been demonstrated that factors like wire mesh size, anchorage types, eccentric loading, and prestress levels affect the stiffness and failure behavior of slabs and columns. This highlights the fact that load-deflection responses in corroded reinforced concrete structures are multifactorial [12,15,17,53].

7. Failure mode observations

7.1. Failure modes in unstrengthened specimens

Unstrengthened slabs exhibited ductile behavior with significant flexural deflections. Large flexural cracks were observed in the tension zone, while no shear cracks were noted due to the low height and large shear span. The first flexural crack appeared at 17 kN [53]. Failure occurred primarily due to yielding of reinforcement steel, followed by shear crack propagation and concrete crushing in both tension and compression zones. Corroded slabs exhibited brittle behavior with cracks propagating radially from the impact points, transitioning to punching shear failure. Severe longitudinal cracks were also noted with increasing corrosion levels [8,11]. Failure in unstrengthened beams typically followed an under-reinforced pattern: tensile steel yielding was followed by concrete crushing [16]. Low-corrosion beams exhibited ductile failure with gradual deflection, while high-corrosion beams failed abruptly due to bond failure and concrete crushing [16]. Failure in unstrengthened columns was characterized by crushing of concrete and buckling of longitudinal steel bars. This brittle failure occurred within single or multiple stirrup spacings [48].

7.2. Failure modes in FRP-strengthened systems

Strengthened slabs generally failed due to CFRP rupture after tensile steel yielding. The CFRP systems demonstrated excellent flexural strengthening capabilities, increasing load-carrying capacities [15,56]. Crack localization was observed in areas between FRP strips, which allowed the slab to sustain loading even after yielding [25]. Strengthened beams failed progressively, starting with debonding at adhesive interfaces, followed by CFRP laminate rupture [1,27]. Beams with multiple CFRP layers demonstrated improved performance. Two-layer systems primarily failed at the interface, while three-layer systems failed due to concrete crushing on the "strong" side [17]. CFRP jackets improved ductility, allowing greater lateral deformations before buckling. These systems provided enhanced restraint against longitudinal bar buckling [12]. GFRP fabrics effectively controlled crack widths, reducing them by 35%–45% in corroded specimens. This minimized crack propagation and structural degradation [7,12]. Hybrid strengthening systems reduced interfacial failures, such as debonding and delamination, and effectively prevented steel rebar rupture in corroded beams [28].

7.3. Failure modes in cementitious composite systems

In Cementitious Fiber Reinforced Composite Material (C-FRCM) strengthened columns avoided concrete spalling and exhibited controlled crack propagation due to the confinement effect [22].

Similarly, in UHPFRC (Ultra High-Performance Fiber Reinforced Concrete): Failure included concrete cover spalling, debonding of UHPFRC jackets, and fiber pull-out. These systems demonstrated enhanced structural integrity by absorbing circumferential deformation [52]. ECC strengthened specimens exhibited tensile cracks and significant plastic deformation in tension zones. These failure modes aligned well with numerical predictions [4].

7.4. Ferrocement jacketing systems

Ferrocement jackets with chemical anchors delayed debonding more effectively than mechanical anchors. This provided enhanced resistance against structural failures [53].

7.5. Carbon epoxy and e-glass/epoxy systems

Slabs strengthened with carbon epoxy exhibited localized shear failure near unstrengthened portions at the edges. Bond lines remained intact, demonstrating good adhesion. E-Glass epoxy systems failed primarily due to laminate debonding, leading to sudden load capacity drops. Variability in workmanship was noted as a contributing factor [25]. In epoxy-strengthened samples, debonding at the interface was seen as the dominant failure mechanism, frequently starting at the rebar concrete interface. This mode of failure is different from FRP-only system, which exhibited flexural failure due to enhanced bonding.

7.6. Corrosion-induced failures

In slab Corrosion led to a transition from punching shear to flexural failure as levels increased. Severe corrosion resulted in wide longitudinal cracks, reducing punching shear resistance [8,26]. In beams Corrosion-induced pitting compromised structural ductility, resulting in abrupt failures. Ultimate load capacities in corroded beams were reduced by 50% [16,20]. For columns Corrosion caused detachment of concrete covers and laminate tearing. Crack widths increased with higher corrosion levels, contributing to severe degradation [7].

7.7. Failure mode description

A thorough analysis of the failure modes of reinforced concrete (RC) elements under varied circumstances shows that loading scenarios, corrosion, and retrofitting techniques all have a significant impact on structural behavior. As demonstrated by corroded slab-column connections and beams where crack propagation and failure zone size increased with corrosion degree, corrosion dramatically changes failure mechanisms, frequently causing them to shift from ductile flexural failures to brittle punching shear failures [2,3,8]. Stirrup corrosion decreased shear capacity in beams, causing brittle or changed mechanical behaviour [2], whereas higher corrosion levels in slabs caused shifts from punching to flexural failure [8]. Due to decreased cover integrity, corroded columns displayed early cracking and spalling; CFRP confinement proved more successful than GFRP in limiting damage [7]. Additionally, studies showed that loading rate affected the type of failure and bond behavior, favoring punching shear over flexural failure at higher rates [11]. Retrofitting methods like CFRP jacketing increased ductility and slowed the spread of cracks in repaired beams and columns, but debonding was still a major failure mode [1,55]. Although debonding and cover separation were common, slabs retrofitted with ferrocement or UHPC layers also showed increased strength and ductility [9,53]. While ultra-high performance concrete (UHPC) and CFRP greatly improved load-carrying capacity and delayed failure, they were unable to completely prevent failure when strain localization or material incompatibility occurred, according to experimental and finite element analyses [12,15,55]. In every study, tensile bar yielding and concrete crushing caused unreinforced and under-reinforced elements to fail in flexure, whereas strengthened elements displayed intricate interactions that resulted in altered failure mechanisms [16,25]. These results highlight the importance of corrosion, strengthening techniques, and reinforcement detailing in controlling the failure modes of reinforced concrete structures, and the need for more research on advanced and hybrid materials under practical service conditions.

Numerous studies have found a variety of failure mechanisms in corroded and strengthened RC members, influenced by corrosion severity, reinforcement configurations, and strengthening techniques. In uncorroded reference beams RN1 and RN2, typical flexural failures were documented, where the compressive side of the beam was crushed by concrete. Corrosion, however, caused variability in failure patterns, necessitating a localized evaluation of the severity of damage [20]. Slabs with various strengthening configurations showed a variety of behaviors, from brittle rupture of composite fabrics and debonding of strengthening materials to shear failure at stress concentration zones, while control slabs showed ductile flexural failures as a result of reinforcement yielding [19]. Advanced techniques like Cementitious Fiber Reinforced Composite Material (C-FRCM), Impressed Current Cathodic Protection-Structural Strengthening (ICCP-SS), and hybrid methods partially mitigated the complex failure modes caused by corrosion-induced degradation of steel in RC columns and joints, including spalling, shear-

flexural interaction, and expansion-induced cracking [22,26]. Depending on the configuration and degree of damage, studies also showed how CFRP, TRC, BFRP, ECC, UHPFRC, and other advanced materials affected failure by changing crack patterns, improving confinement, postponing debonding, and shifting failure from flexural to shear modes or vice versa. The usefulness of numerical models in forecasting performance under various corrosion and strengthening conditions has been highlighted by their strong agreement with experimental failure modes [4,6,17,23,48,52,57,58]. The body of evidence shows that although flexural failure is still common in many unstrengthened or mildly corroded members, corrosion frequently causes brittle or mixed failure modes, which can be postponed or redirected with the help of efficient strengthening techniques [13,15,18,54].

The table 5 shows the comparative analysis of failure modes.

Table 5. Comparative analysis of failure modes across strengthening systems.

Strengthening System	Failure Mode Description	Ductility	Crack Propagation	Ultimate Load Capacity	References
Unstrengthened RC Members	Yielding of steel, flexural cracks, concrete crushing, brittle punching shear in corroded elements	Low–Moderate	Severe, radial, longitudinal	Decreased (up to -50%)	[2,8,11,53,55]
FRP Systems (CFRP/GFRP)	Debonding at interface, FRP rupture, concrete crushing; improved restraint on buckling	High	Localized, controlled	High	[1,7,12,15,17,25,27,28]
Hybrid Systems (CFRP-GFRP, etc.)	Reduced debonding, improved confinement, and prevention of steel rupture	High	Well-restrained	High	[12,28]
UHPFRC Jackets	Cover spalling, fibre pull-out, jacket debonding, deformation absorption through confinement	Moderate–High	Minimized	High	[52]
ECC with BFRP Grids	Plastic deformation, concrete support; delay in brittle failure	High	Delayed propagation	High	[4]
C-FRCM Composites	Avoided spalling, confinement-induced stability, consistent load transfer	High	Controlled	Moderate–High	[22]
ICCP-SS (C-FRCM + Cathodic)	Reduced crack widths, anode-cathode protection system, uniform potential stabilization	Moderate–High	Greatly reduced	Moderate–High	[59]
Ferrocement Jackets	Delayed debonding; better anchorage with chemical anchors	Moderate	Moderate	Moderate	[9,53]
Carbon/E-Glass Epoxy	Localized shear (carbonyl epoxy), laminate debonding (E-glass); workmanship sensitive	Moderate	Debonding prominent	Variable	[25]
NSM-CFRP	Interface debonding controlled, improved prestressing, anchorage sensitive	High	Localized	High	[15]
Basalt Textile (BFRP/BTRM)	Delayed failure, improved flexural capacity; no end anchoring	Moderate–High	Slowed, layered pattern	Moderate–High	[57]
CFRP Rods + Steel Plates	Strong composite bond: rod pull-out controlled; end anchorage critical	High	Minimized	High	[5]
CFRP Strips	High stiffness/strength; surface prep critical; debonding in poorly prepared zones	Moderate–High	Localized	High	[48]
CFRP Wet Layup (Various Layers)	Layer-based performance; more layers = higher failure capacity; common debonding without U-wraps	Moderate–High	Reduced with wrap techniques	High	[1,15,20,60]
CFL + Steel Plates	Good anchorage, epoxy bonding; failure depends on bolt layout and overlap region	High	Well-controlled	High	[61]

8. Results

The recent developments in advanced materials and techniques have led to the development of innovative solutions capable of substantially improving structural performance. After being equipped with ferrocement jackets, for example, Peak load and deflection increased by as much as 49% and 109%, respectively, whereas energy dissipated increased by 174% [53]. The CFRP and GFRP also have significant effects on the repair of the RC slabs and columns, with CFRP showed more efficiently in flexural strength (2-7 times higher than the original) and lateral deformation [53]. It was also found in studies that the presence of corrosion changes the mode of failure from flexural to shear failure, emphasizing the importance of tailored strengthening techniques like the critical shear crack theory (CSCT) model [3,8]. Considerable increases in ultimate loads, stiffness, and cracking resistance were achieved using techniques like ultra-high-performance concrete (UHPC) layers, Near Surface Mounted (NSM) FRP laminates, and hybrid CFRP-GFRP laminates [16,28,56]. However, the advantages of these approaches were lost in intense corrosion, and multiple layers or hybrid approaches may be needed [2,28]. In this study, the analytical models always matched the experimental results, which can provide people with reliable prediction for the structural behavior. The paper underscores the efficacy of CFRP-based methods but also highlights gaps in addressing deformation capacities, recommending further investigation into hybrid systems and composite materials [48,57].

Table 6. Findings from the different strengthening techniques.

Material	Strengthening Technique	Key Findings and Improvements	Reference
Ferrocement	Ferrocement Jackets	Increased peak load by 49% and ultimate deflection by 109%.	[53]
		Dissipated energy increased by 174%, significantly improving ductility.	
Fiber-Reinforced Polymer (FRP)	Externally Bonded (EB) FRP Sheets	Delayed cracking and enhanced resistance to shear cracks in slabs.	[62]
		Improved punching shear capacity, retaining 30% of ultimate strength without cracking.	[62]
	CFRP/GFRP Fabrics	Increased flexural strength and lateral deformation in columns.	[7]
		CFRP was more effective than GFRP at higher corrosion levels.	
	Near-Surface Mounted (NSM) FRP Bars	Slabs using prestressed CFRP laminates had up to 400% increases in cracking, service, and ultimate loads.	[15,63]
	CFRP Jackets	Restored load capacity in beams and columns, even for specimens with 20% corrosion.	[5,12]
		Enhanced ductility and confined concrete effectively under eccentric loads.	
	Hybrid Systems (CFRP + GFRP)	Achieved 60% strength recovery in corroded beams using CFRP-GFRP laminates.	[28]
		Improved fatigue life and delayed crack growth in corroded steel plates.	
Ultra-High-Performance Concrete (UHPC)	UHPC Layers	Increased flexural strength by up to 63% and stiffness by 112% in beams.	[16]
		Load-carrying capacity improved by up to 46% for RC columns with UHPC jackets.	[52]
		Reduced corrosion rates significantly from 3.02% to as low as 0.35%.	
Engineered Cementitious Composite (ECC)	ECC Bonding Layers	UHTCC bonding layers enhanced load-bearing capacity of slabs by up to 120.92% and improved toughness by 166%.	[21]
Basalt Fiber Reinforced Concrete (BFRC)	Basalt Grids and Fibers	Flexural capacity increased by 63% in beams using MiniBars™.	[4,6]
		Improved ductility with delayed load degradation during the softening stage.	

Cementitious Fiber Reinforced Composite Material (C-FRCM)	C-FRCM Wrapping Systems	Increased bending capacity, stiffness, and energy dissipation in beams and columns.	[23,61]
Two layers provided similar performance to three layers, optimizing material use.			
Hybrid Systems	ICCP-SS (Impressed Current Cathodic Protection and Structural Strengthening)	ICCP-SS system enhanced load capacity and mitigated corrosion progression effectively.	[22,23]
Combined effect of ICCP and carbon-fabric reinforcement increased ductility and reduced delamination.			
Textile Reinforced Concrete (TRC)	TRC Strengthening Layers	Restored shear strength and stiffness in corroded beams, with failure shifting from shear cracking to crushing in strong zones.	[17]

9. Practical implementation challenges, cost considerations, and selection guidance

The choice of an effective strengthening method for corroded reinforced concrete (RC) members involves careful consideration of numerous practical, economic, and contextual issues. In spite of major developments in the materials and application approaches, implementation of these methods in real-world conditions is frequently constrained by site conditions, corrosion level, structural use, and budgetary constraints.

9.1. Practical implementation challenges

Every strengthening method has its own set of implementation challenges, which can influence constructability and long-term performance:

- **Surface Preparation:** Thorough surface roughening, cleaning, and moisture conditioning are necessary for technique including CFRP wet layup, NSM-CFRP, and ICCO systems, Inadequate preparation may result in poor bond performance or early debonding.
- **Anchorage Requirements:** For CFRP rods, CFRP anchors, and hybrid CFRP-GFRP systems, specific anchorages such as steel plates and bolts are required, making installation more complicated and labour intensive.
- **Environmental Sensitivity:** The BFRP/BTRM and Engineered Cementitious Composite-Fibre Reinforced Polymers (ECC-FRP) systems are not suitable for remote or open-exposure locations since they require controlled curing and protection (such as burlap wrapping or wet curing).
- **Complicated Application Processes:** Methods like hybrid prefabricated Cementitious Fiber Reinforced Composite Material (C-FRCM) plates and impressed current cathodic protection-structural strengthening (ICCP-SS) require professional workers and multi-stage preparation (e.g., anodic polarization, electrode installation), increasing the risk of construction errors and delays.
- **Structural Access:** Access is limited by techniques like jacketing with UHPFRC or NSM bar embedment, particularly in structures that are small or occupied or when columns or beams are completely embedded.

9.2. Cost factors

The comparative cost of strengthening systems differs extensively and needs to be evaluated in material, labor, and long-term maintenance expenses:

- **Expensive Systems:** Hybrid Impressed Current Cathodic Protection-Structural Strengthening (ICCP-SS), UHPFRC jacketing, and Engineered Cementitious Composite-Fibre Reinforced Polymers (ECC-FRP)

systems provide superior durability and corrosion protection at high initial cost because of the expense of materials, expert labor, and machinery (e.g., polarization units).

- **Medium-Cost Systems** Module-based Cementitious Fiber Reinforced Composite Material (C-FRCM) plates, CFRP laminates, and NSM bars offer sufficient performance at a lower cost than the first two varieties. Prefabrication and modularity reduce labor costs on the job site, but they can increase transportation and curing costs.

- **Budget-Friendly Choices:** Ferrocement jackets, GFRP fabrics, and wet layup FRP wraps are cost-effective and less complicated to install in low- to medium-damage areas.

- **Concealed Lifecycle Costs:** Long-term maintenance, resilience to adverse environments (i.e., sea exposure), and reapplication frequency (e.g., BTRM or GFRP in highly corrosive locations) should all be taken into consideration when making decisions.

9.3. Decision-making factors

When deciding on a strengthening method, the following practical considerations also need to be evaluated:

- **Emergency of Repair:** Wet layup CFRP or GFRP can be opted for emergency use on account of ease of deployment.

- **Availability of Skilled Manpower:** Impressed Current Cathodic Protection (ICCP), Engineered Cementitious Composite (ECC), and textile-reinforced concrete (TRC)-based technologies require skilled application; less complex FRP or GFRP techniques might be more desirable where there is a scarcity of skilled workforce.

- **Compatibility with Current Material:** Compatibility in thermal expansion, bonding, and permeability is crucial. ultra-high performance concrete (UHPC) or Engineered Cementitious Composite (ECC) cannot be compatible with all NSC types without surface conditioning.

- **Structural Redundancy and Function:** Beams and slabs can utilize flexural reinforcements, whereas columns require confinement reinforcement type should be the same as the failure mode.

- **Service Life Objectives:** ICCP and hybrid systems are best for structures intended to have a service life over 30–50 years under severe environments.

10. Limitations

- Material incompatibility and debonding at the FRP concrete contact continue to be a major issue.
- Performance under combined mechanical-environmental loading conditions (e.g., seismic + corrosion) is still inadequately explored.
- Many existing studies lack long-term performance data under realistic service conditions.

11. Research gaps and future directions

Despite the significant advancements in strengthening techniques for corroded RC structures, several critical research gaps remain. These gaps can be organized into the following thematic areas:

11.1. Material innovation and performance

- Beyond CFRP and GFRP: Polymer fabric alternatives and hybrid fibre composites are being least explored. New materials like basalt fibres, textile-reinforced concrete (TRC), and ultra-high toughness cementitious composites (UHTCC) need to be researched for long-term performance.
- Performance under Harsh Conditions: Comprehensive studies on how strengthening systems (e.g., CFRP, UHPC, TRC) behave under marine, seismic, and multi-hazard conditions are lacking.
- Prestressed FRP Systems: Impact of prestressing levels and methods on the response of BFRP-strengthened slabs requires careful experimental verification.

11.2. Modelling and predictive simulation

Enhanced FE Modelling: Present finite element models tend to simplify intricate deterioration mechanisms. There is a necessity to:

1. Improve corrosion-damage simulation and crack growth in FRP-strengthened steel and concrete.
2. Embed time-dependent impacts such as fatigue and weathering degradation.
3. Create multi-scale models connecting material deterioration to structural response.

Cost and Performance Optimization: Future models must consider the cost-effectiveness and feasibility of various strengthening approaches at a range of corrosion levels.

11.3. Bonding, interface, and anchorage mechanisms

- Interface Durability: Development should center on enhancing the bond between FRP and corroded concrete, particularly under cyclic or wet-dry conditions.
- Examine adhesives, surface treatments, and CFRP rod anchoring methods (e.g., chemical anchors).
- Mitigation of Debonding: Experimental tests must be conducted to minimize debonding failure in NSM and externally bonded systems, particularly for retrofitted continuous beams and columns.

11.4. Structural design and codification

- Design Criteria for Retrofitted Systems: Codes currently available do not have provisions for corrosion-damaged and retrofitted continuous beams. New standards are necessary to:
- Estimate post-repair capacity.
- Deal with structural behaviour under shear-dominant damage in damaged beams.
- Hybrid Strengthening Methods: More proof of ICCP-SS, ECC-FRP, and UHPC-GFRP hybrids is required to offer simultaneous benefits of mechanical reinforcement and corrosion protection.

11.5. Health monitoring and real-time assessment

- New Monitoring Technologies: Use real-time damage detection with:
- Acoustic Emission (AE) methods for early crack and delamination monitoring.
- Smart sensors and digital twin platforms for long-term performance tracking.
- Corrosion-Bond Interaction: It is still uninvestigated and very important to determine how varying degrees of corrosion affect the bond behaviour in strengthened RC members.

12. Recommendations for practitioners

- CFRP or GFRP strengthening can restore up to 32% of lost strength and 52% of deflection capacity for low to moderate corrosion level ($\leq 20\%$).
- UHPC overlays or prestressed CFRP laminates, which can increase load capacity by up to 134%, should be used in areas with high corrosion levels ($>30\%$).
- Use CFRP laminates, NSM-BFRP bars, or UHPC overlays for slab and beam strengthening to restore 45–162% in strength.
- Strengthen columns with CFRP or UHPFRC jacketing for enhanced ductility and energy dissipation of up to 239%.
- Use 2–3 layers of CFRP for higher structural performance; however, check for debonding and do not over-stiffen.
- Utilize prestressed CFRP when high load carrying capacity is essential, but do not use in members that require greater ductility or deformability.
- In seismic or impact-susceptible areas, use ECC with basalt fibers, GFRP, or UHPFRC to increase post-cracking energy absorption by 130%.
- Implement hybrid CFRP-UHPC or C-FRCM systems to control brittle modes of failure and improve ductility for highly corroded members.
- Use TRM, UHPC jacketing, or NSM-FRP system configurations to restore or achieve initial stiffness 33% improvement in stiffness has been recorded.
- Enforce suitable surface treatment and bonding practices, particularly for FRP systems, to prevent early debonding.
- In buildings subject to marine or chloride exposure, use ICCP-SS hybrid systems for improved corrosion protection.
- Ferrocement jacketing and NSM-BFRP processes provide practical and affordable solutions for low to moderate damage applications.

13. Conclusions

This review highlights the impact of advanced strengthening techniques on the rehabilitation of corroded reinforced concrete (RC) structures. Key findings are.

- The load carrying capacity, ductility, and seismic behavior of corroded RC Slabs, beams, and Columns are significantly improved by CFRP, GFRP, and Hybrid systems.
- For externally bonded FRP systems, surface preparation such as grinding, grooving, and epoxy mortar is essential to ensuring the bond's effectiveness.
- Prestressed CFRP laminates and ultra high-performance concrete (UHPC) overlays optimize flexural performance, stiffness, and crack resistance.
- Particularly in chloride or marine situations, impress current cathodic protection structural strengthening (ICCP-SS) systems offer both active corrosion protection and structural strengthening.
- NSM bars and CFRP + steel plates are examples of hybrid approaches that demonstrate exceptional capacity to manage complex failure patterns.
- Experimental results are validated by numerical models, which faithfully replicate structural behaviour such as failure mechanisms, deflection patterns, and stiffness deterioration.

Funding

This research did not receive any specific grant from funding agencies in the public, commercial, or not-for-profit sectors.

Conflict of Interest

The authors declare that they have no known competing financial interests or personal relationships that could have appeared to influence the work reported in this paper.

Availability of data

Not applicable

Author Contributions

Mankare Ulka: Conceptualization, Formal analysis, Methodology, Validation, Visualization, Data curation, Investigation, Writing – original draft, Writing – review & editing.

Viswanathan T S: Conceptualization, Formal analysis, Methodology, Validation, Visualization, Writing – review & editing, Project administration, Resources, Supervision.

References

- [1] Al-Mashgari HAY, Hejazi F, Alkhateeb MY. Retrofitting of corroded reinforced concrete beams in flexure using CFRP rods and anchor bolt. *Structures* 2021;29:1819–27. <https://doi.org/10.1016/j.istruc.2020.12.047>.
- [2] Chen S, Lyu H, Wang L, Zhang X. Research on Arch Effect and CFRP Strengthening Effect of RC Beams with Corroded Stirrups. *KSCE J Civ Eng* 2018;22:5026–34. <https://doi.org/10.1007/s12205-017-1236-z>.
- [3] Qian K, Li J-S, Huang T, Weng Y-H, Deng X-F. Punching shear strength of corroded reinforced concrete slab-column connections. *J Build Eng* 2022;45:103489. <https://doi.org/10.1016/j.jobe.2021.103489>.
- [4] Zhang Z, Guo X, Yang Z, Ji J, Sun Q, Tian P, et al. Flexural behavior of the corroded RC beams strengthened with BFRP grid-reinforced ECC. *Structures* 2023;58:105541. <https://doi.org/10.1016/j.istruc.2023.105541>.
- [5] Xu Y-Y, Huang J-Q. Cyclic performance of corroded reinforced concrete short columns strengthened using carbon fiber-reinforced polymer. *Constr Build Mater* 2020;247:118548. <https://doi.org/10.1016/j.conbuildmat.2020.118548>.
- [6] Zhang Z, Wu X, Sun Q, Tian P, Hu G. Compressive behavior of corroded reinforced concrete columns strengthened with BFRP reinforced ECC in marine environment. *Ocean Eng* 2023;279:114533. <https://doi.org/10.1016/j.oceaneng.2023.114533>.
- [7] Karimipour A, Edalati M. Retrofitting of the corroded reinforced concrete columns with CFRP and GFRP fabrics under different corrosion levels. *Eng Struct* 2021;228:111523. <https://doi.org/10.1016/j.engstruct.2020.111523>.
- [8] Yang Z, Ma J, Li B. Investigating the impact of corrosion on behavior and failure modes of reinforced concrete slabs: An experimental and analytical study. *Eng Struct* 2024;321:118983. <https://doi.org/10.1016/j.engstruct.2024.118983>.
- [9] Sun X, Gong Z, Zuo Y, Hu J, Li Y, Wu H, et al. Flexural behavior of the hollow slab girders strengthened with ultra-high performance concrete: Field full-scale experiment and analysis. *Constr Build Mater* 2023;408:133608. <https://doi.org/10.1016/j.conbuildmat.2023.133608>.
- [10] Feng R, Liu P, Zhang J, Wang F, Xu Y, Zhu J-H. Bending behaviour of corroded RC continuous beams with C-FRCM strengthening system. *J Build Eng* 2022;60:105229. <https://doi.org/10.1016/j.jobe.2022.105229>.
- [11] Daneshvar K, Moradi MJ, Ahmadi K, Hajiloo H. Strengthening of corroded reinforced concrete slabs under multi-impact loading: Experimental results and numerical analysis. *Constr Build Mater* 2021;284:122650. <https://doi.org/10.1016/j.conbuildmat.2021.122650>.

- [12] Chotickai P, Tongya P, Jantharaksa S. Performance of corroded rectangular RC columns strengthened with CFRP composite under eccentric loading. *Constr Build Mater* 2021;268:121134. <https://doi.org/10.1016/j.conbuildmat.2020.121134>.
- [13] Yu X-Y, Jiang C, Zhang W-P. Failure mode-based calculation method for bending bearing capacities of corroded RC beams strengthened with CFRP sheets. *Eng Struct* 2022;271:114946. <https://doi.org/10.1016/j.engstruct.2022.114946>.
- [14] Aljidda O, El Refai A, Alnahhal W. Experimental and analytical investigation on the use of NSM-BFRP and NSM-GFRP bars in strengthening corrosion-damaged RC slabs. *Compos Struct* 2023;322:117428. <https://doi.org/10.1016/j.compstruct.2023.117428>.
- [15] Mostakhdemin Hosseini MR, Dias SJE, Barros JAO. Flexural strengthening of reinforced low strength concrete slabs using prestressed NSM CFRP laminates. *Compos Part B Eng* 2016;90:14–29. <https://doi.org/10.1016/j.compositesb.2015.11.028>.
- [16] Al-Huri MA, Ahmad S, Al-Osta MA, Al-Gadhib AH, Kharma KM. Performance of corroded RC beams strengthened in flexure using UHPC: Effect of configuration and thickness of the UHPC layers. *Eng Struct* 2023;292:116519. <https://doi.org/10.1016/j.engstruct.2023.116519>.
- [17] Ngo DQ, Nguyen HC, Dinh HT, Nguyen DT, Mai DL. Effectiveness of carbon textile reinforced concrete in shear strengthening short-span corroded reinforced concrete beams. *Case Stud Constr Mater* 2022;16. <https://doi.org/10.1016/j.cscm.2022.e00932>.
- [18] Biswas RK, Misawa T, Saito T, Iwanami M. An experimental and numerical investigation on the flexural strengthening of full-scale corrosion-damaged RC columns using UHPC layers. *Constr Build Mater* 2024;449. <https://doi.org/10.1016/j.conbuildmat.2024.138269>.
- [19] Zheng X, Wan B, Huang P, Huang J. Experimental study of hybrid strengthening technique using carbon fiber laminates and steel plates for reinforced concrete slabs. *Constr Build Mater* 2019;210:324–37. <https://doi.org/10.1016/j.conbuildmat.2019.03.100>.
- [20] Yang J, Haghani R, Blanksvärd T, Lundgren K. Experimental study of FRP-strengthened concrete beams with corroded reinforcement. *Constr Build Mater* 2021;301:124076. <https://doi.org/10.1016/j.conbuildmat.2021.124076>.
- [21] Xu S, Xie H, Li Q, Hong C, Liu J, Wang Q. Bending performance of RC slabs strengthened by CFRP sheets using sprayed UHTCC as bonding layer: Experimental study and theoretical analysis. *Eng Struct* 2023;292:116575. <https://doi.org/10.1016/j.engstruct.2023.116575>.
- [22] Feng R, Zhang J, Li Y, Zhu J-H. Experimental study on hysteretic behavior for corroded circular RC columns retrofitted by ICCP-SS. *Structures* 2022;35:421–35. <https://doi.org/10.1016/j.istruc.2021.10.039>.
- [23] Feng R, He X, Wang F, Zeng J-J, Zhu J-H. Experimental analysis of corroded RC continuous beams rehabilitated by ICCP-SS under unsymmetrical loading. *Structures* 2022;46:1171–88. <https://doi.org/10.1016/j.istruc.2022.10.110>.
- [24] Feng R, Li Y, Zhu J-H, Xing F. Behavior of corroded circular RC columns strengthened by C-FRCM under cyclic loading. *Eng Struct* 2021;226:111311. <https://doi.org/10.1016/j.engstruct.2020.111311>.
- [25] Mosallam AS, Mosalam KM. Strengthening of two-way concrete slabs with FRP composite laminates. vol. 17. 2003.
- [26] Gomaa AM, Lotfy EM, Khafaga SA, Hosny S, Ahmed MA. Experimental, numerical, and theoretical study of punching shear capacity of corroded reinforced concrete slab-column joints. *Eng Struct* 2023;289:116280. <https://doi.org/10.1016/j.engstruct.2023.116280>.
- [27] Kharma KM, Ahmad S, Al-Osta MA, Maslehuddin M, Al-Huri M, Khalid H, et al. Experimental and analytical study on the effect of different repairing and strengthening strategies on flexural performance of corroded RC beams. *Structures* 2022;46:336–52. <https://doi.org/10.1016/j.istruc.2022.10.078>.
- [28] Ghous Sohail M, Wasee M, Al Nuaimi N, Alnahhal W, Hassan MK. Behavior of artificially corroded RC beams strengthened with CFRP and hybrid CFRP-GFRP laminates. *Eng Struct* 2022;272:114827. <https://doi.org/10.1016/j.engstruct.2022.114827>.
- [29] Abas Golham M, Al-Ahmed AHA. Behavior of GFRP reinforced concrete slabs with openings strengthened by CFRP strips. *Results Eng* 2023;18:101033. <https://doi.org/10.1016/j.rineng.2023.101033>.

- [30] Khanahmadi M. A cutting-edge framework for damage-sensitive feature extraction leveraging modal dynamic flexibility in signal processing-driven structural health monitoring. *Thin-Walled Struct* 2025;216. <https://doi.org/10.1016/j.tws.2025.113617>.
- [31] Khanahmadi M. An effective vibration-based feature extraction method for single and multiple damage localization in thin-walled plates using one-dimensional wavelet transform: A numerical and experimental study. *Thin-Walled Struct* 2024;204:112288. <https://doi.org/10.1016/j.tws.2024.112288>.
- [32] Naderpour H, Fakharian P. A synthesis of peak picking method and wavelet packet transform for structural modal identification. *KSCE J Civ Eng* 2016;20:2859–67. <https://doi.org/10.1007/s12205-016-0523-4>.
- [33] 62. View of A review of the application of the simulated annealing algorithm in structural health monitoring (1995-2021).pdf n.d.
- [34] Guide for the design and construction of externally bonded FRP systems for strengthening concrete structures. American Concrete Institute; 2017.
- [35] SikaWrap®-530 C WOVEN UNIDIRECTIONAL CARBON FIBRE FABRIC, DESIGNED FOR STRUCTURAL STRENGTHEN-ING APPLICATIONS AS PART OF THE SIKA® STRENGTHENING SYSTEM. 2017.
- [36] Sikadur®-300., 2017.
- [37] Kalfat R, Al-Mahaidi R, Smith ST. Anchorage Devices Used to Improve the Performance of Reinforced Concrete Beams Retrofitted with FRP Composites: State-of-the-Art Review. *J Compos Constr* 2013;17:14–33. [https://doi.org/10.1061/\(ASCE\)CC.1943-5614.0000276](https://doi.org/10.1061/(ASCE)CC.1943-5614.0000276).
- [38] Spadea G, Bencardino F, Sorrenti F, Swamy RN. Structural effectiveness of FRP materials in strengthening RC beams. *Eng Struct* 2015;99:631–41. <https://doi.org/10.1016/j.engstruct.2015.05.021>.
- [39] MARK SHAW. Technical Information manual SikaWrap® wet application, 2016.
- [40] Pan T, Zheng Y, Zhou Y, Luo W, Xu X, Hou C, et al. Damage pattern recognition for corroded beams strengthened by CFRP anchorage system based on acoustic emission techniques. *Constr Build Mater* 2023;406:133474. <https://doi.org/10.1016/j.conbuildmat.2023.133474>.
- [41] Orton SL, Jirsa JO, Bayrak O. Design Considerations of Carbon Fiber Anchors. *J Compos Constr* 2008;12:608–16. [https://doi.org/10.1061/\(ASCE\)1090-0268\(2008\)12:6\(608\)](https://doi.org/10.1061/(ASCE)1090-0268(2008)12:6(608)).
- [42] Llauradó PV, Fernández-Gómez J, González Ramos FJ. Influence of geometrical and installation parameters on performance of CFRP anchors. *Compos Struct* 2017;176:105–16. <https://doi.org/10.1016/j.compstruct.2017.05.035>.
- [43] Włodarczyk M, Jędrzejewski I. Concrete Slabs Strengthened with Basalt Fibres - Experimental Tests Results. *Procedia Eng.*, vol. 153, Elsevier Ltd; 2016, p. 866–73. <https://doi.org/10.1016/j.proeng.2016.08.200>.
- [44] Chen C, Li X, Zhao D, Huang Z, Sui L, Xing F, et al. Mechanism of surface preparation on FRP-Concrete bond performance: A quantitative study. *Compos Part B Eng* 2019;163:193–206. <https://doi.org/10.1016/j.compositesb.2018.11.027>.
- [45] Hosseini A, Mostofinejad D. Experimental investigation into bond behavior of CFRP sheets attached to concrete using EBR and EBROG techniques. *Compos Part B Eng* 2013;51:130–9. <https://doi.org/10.1016/j.compositesb.2013.03.003>.
- [46] Tajmir-Riahi A, Moshiri N, Mostofinejad D. Bond mechanism of EBROG method using a single groove to attach CFRP sheets on concrete. *Constr Build Mater* 2019;197:693–704. <https://doi.org/10.1016/j.conbuildmat.2018.11.204>.
- [47] Chen C, Li X, Wang X, Sui L, Xing F, Li D, et al. Effect of transverse groove on bond behavior of FRP-concrete interface: Experimental study, image analysis and design. *Compos Part B Eng* 2019;161:205–19. <https://doi.org/10.1016/j.compositesb.2018.10.072>.
- [48] Li N, Li W, Lu Y, Li S. Corroded reinforced concrete columns strengthened with basalt fibre reinforced ECC under axial compression. *Compos Struct* 2023;303:116328. <https://doi.org/10.1016/j.compstruct.2022.116328>.
- [49] Zhao B, Taucer F, Rossetto T. Field investigation on the performance of building structures during the 12 May 2008 Wenchuan earthquake in China. *Eng Struct* 2009;31:1707–23. <https://doi.org/10.1016/j.engstruct.2009.02.039>.

- [50] Wang ZY, Wang DY, Sheikh SA, Liu JT. Seismic Performance of FRP-Confined Circular RC Columns. *Adv. FRP Compos. Civ. Eng.*, Berlin, Heidelberg: Springer Berlin Heidelberg; 2011, p. 810–4. https://doi.org/10.1007/978-3-642-17487-2_178.
- [51] Chinese Code. Technical Specification for Strengthening Concrete Structures with Carbon Fiber Reinforced Polymer Laminate 2007.
- [52] Tang J-P, Feng R, Quach W-M, Zeng J-J. Axial compressive behaviour of simulated corrosion-damaged RC columns retrofitted with UHPFRC jackets subjected to dry-wet cycling condition. *Constr Build Mater* 2024;424:135956. <https://doi.org/10.1016/j.conbuildmat.2024.135956>.
- [53] Joyklad P, Krishna Gadagamma C, Maneengamlert B, Nawaz A, Ejaz A, Hussain Q, et al. Structural behavior of RC one-way slabs strengthened with ferrocement and FRP composites. *Eng Fail Anal* 2024;161:108328. <https://doi.org/10.1016/j.engfailanal.2024.108328>.
- [54] Fang L, Zhou Y, Yi D, Yi W. Experimental study on flexural capacity of corroded rc slabs reinforced with basalt fiber textile. *Appl Sci* 2021;11:1–25. <https://doi.org/10.3390/app11010144>.
- [55] Ghayeb HH, Atea RS, Al-Kannoon MAA, Lee FW, Wong LS, Mo KH. Performance of reinforced concrete flat slab strengthened with CFRP for punching shear. *Case Stud Constr Mater* 2023;18. <https://doi.org/10.1016/j.cscm.2022.e01801>.
- [56] Mostakhdemin Hosseini MR, Dias SJE, Barros JAO. Effectiveness of prestressed NSM CFRP laminates for the flexural strengthening of RC slabs. *Compos Struct* 2014;111:249–58. <https://doi.org/10.1016/j.compstruct.2013.12.018>.
- [57] Li A, Xu S, Wang Y, Wu C, Nie B. Fatigue behavior of corroded steel plates strengthened with CFRP plates. *Constr Build Mater* 2022;314:125707. <https://doi.org/10.1016/j.conbuildmat.2021.125707>.
- [58] He W, Wang X, Ding L, Wu Z. Efficiency of different BFRP-based strengthening techniques in improving flexural behavior of RC slabs. *Constr Build Mater* 2021;308:125002. <https://doi.org/10.1016/j.conbuildmat.2021.125002>.
- [59] Cathodic Protection of Steel in Concrete (ISO 12696:2016) BSI Standards Publication. 2017.
- [60] Fang L, Zhou Y, Yi D, Yi W. Experimental Study on Flexural Capacity of Corroded RC Slabs Reinforced with Basalt Fiber Textile. *Appl Sci* 2020;11:144. <https://doi.org/10.3390/app11010144>.
- [61] Feng R, Li Y, Zhu JH, Xing F. Behavior of corroded circular RC columns strengthened by C-FRCM under cyclic loading. *Eng Struct* 2021;226. <https://doi.org/10.1016/j.engstruct.2020.111311>.
- [62] Ghayeb HH, Atea RS, Al-Kannoon MA-A, Lee FW, Wong LS, Mo KH. Performance of reinforced concrete flat slab strengthened with CFRP for punching shear. *Case Stud Constr Mater* 2023;18:e01801. <https://doi.org/10.1016/j.cscm.2022.e01801>.
- [63] Mostakhdemin Hosseini MR, Dias SJE, Barros JAO. Flexural strengthening of reinforced low strength concrete slabs using prestressed NSM CFRP laminates. *Compos Part B Eng* 2016;90:14–29. <https://doi.org/10.1016/j.compositesb.2015.11.028>.